Scenario analysis, management, and optimization of a new Vehicle-to-Micro-Grid (V2μG) network based on off-grid renewable building energy systems

Wang, Bingzheng; Yu, Xiaoli; Xu, Hongming; Wu, Qian; Wang, Lei; Huang, Rui; Li, Zhi; Zhou, Quan

DOI:
10.1016/j.apenergy.2022.119873

Applied Energy 325 (2022) 119873

Contents lists available at ScienceDirect

Applied Energy

journal homepage: www.elsevier.com/locate/apenergy

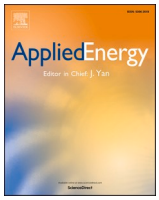

Scenario analysis, management, and optimization of a new Vehicle-to-Micro-Grid (V2μG) network based on off-grid renewable building energy systems

Bingzheng Wang [a,b], Xiaoli Yu [a,b], Hongming Xu [c], Qian Wu [d], Lei Wang [e], Rui Huang [d], Zhi Li [a,b,*,1], Quan Zhou [a,c,*,1]

[a] State Key Laboratory of Clean Energy Utilization, Zhejiang University, Hangzhou 310027, China
[b] Ningbo Research Institute, Zhejiang University, Ningbo 315100, China
[c] School of Engineering, University of Birmingham, B15 2TT, UK
[d] Department of Mechanical Engineering, Zhejiang University City College, 310015, China
[e] Ningbo C.S.I. Power & Machinery Group Co., Ltd., Ningbo 315033, China

HIGHLIGHTS

- A new Vehicle-to-Micro-Grid (V2μG) network is studied in this paper.
- The degradation of BEV batteries can be reduced by introducing FCEVs to the system.
- System configuration, capacity and working modes are optimized using NSGA-II.
- The proposed V2μG network can contribute to 516 t CO_2 emission reduction annually.

ARTICLE INFO

Keywords:
Off-grid building energy system
Vehicle-to-grid network
Electric vehicles
Energy storage

ABSTRACT

To fully exploit the potential of decarburization in the transport sector (e.g., electric vehicles (EV)) and energy sector (e.g., building energy system), this paper proposes a new concept of 'Vehicle-to-Micro-Grid (V2μG) network' that incorporates the off-grid building energy system with flexible power storage/supply provided by battery EVs (BEVs) and fuel cell EVs (FCEVs). The work is conducted with three main contributions: 1) a rule-based energy management strategy is proposed to study the impact of the V2μG interactions on the EV battery degradation; 2) a scenario analysis based on four working modes is conducted to evaluate the energy efficiency, costing, environmental impacts, and component ageing of the proposed V2μG network; 3) the optimum settings for system configuration, capacity, and operation strategy of the V2μG network are obtained by the NSGA-II algorithm. The study suggested that the degradation of lithium-ion batteries in BEV can be reduced by 13% compared to the network without FCEVs. In a community with 160 households and 200 EVs, the optimal V2μG network can reduce carbon dioxide emissions by 515.56 tons annually compared to the conventional off-grid building energy system powered by internal combustion engines.

Abbreviations: AC, absorption chiller; BEV, battery electric vehicle; CCHP, combined cooling, heating, and power; CSE, concentrated solar energy; EES, electric energy storage; EV, electric vehicle; FC, fuel cell; FCEV, fuel cell electric vehicle; HE, heat exchange; HG, hydrogen generation; ICE, internal combustion engine; IEA, international energy agency; NSGA-II, nondominated sorting genetic algorithm II; NZEB, net-zero energy building; O&M, operation and maintenance; PV, photovoltaic; REPG, renewable energy power generation; RES, renewable energy resources; SOC, state of charge; V2G, vehicle-to-grid; V2μG, vehicle-to-Micro-Grid; WHR, waste heat recovery; WT, wind turbine.

* Corresponding authors at: State Key Laboratory of Clean Energy Utilization, Zhejiang University, Hangzhou 310027, China (Z. Li). School of Engineering, University of Birmingham, B15 2TT, UK (Q. Zhou).
E-mail addresses: liz_ym@zju.edu.cn (Z. Li), q.zhou@bham.ac.uk (Q. Zhou).
[1] These authors contributed equally to this article.

https://doi.org/10.1016/j.apenergy.2022.119873
Received 19 April 2022; Received in revised form 16 July 2022; Accepted 16 August 2022
Available online 25 August 2022

Nomenclature

$Age_{d,i}$	degree of battery degradation of each BEV (–)
C	cost ($)
$Cap_{battery}$	capacity of BEV (kWh)
CD_{bp}	carbon dioxide emission of backup power (t)
$CDRR$	carbon dioxide reducing rate (t year^{-1})
CT	carbon tax ($ t^{-1})
$C.V_{deg}$	coefficient of variation of the degradation (–)
DNI	direct normal irradiation (W m^{-2})
E	electricity (kWh)
$H_{V2G,HV}$	additional working hours of FCEV caused by V2G (h)
f_{ICE}	part load of ICE (%)
f_{PV}	attenuation coefficient (–)
F	willingness factor of the vehicle owner to the V2G service (–)
h	height (m)
HHV	molar higher heating value (kJ mol^{-1})
HV	hypervolume
i	interest rate (%)
I	income ($)
k	power temperature coefficient of PV (–)
$LCOE$	levelized cost of electricity ($ kWh^{-1})
L_{cool}	cooling load (kWh h^{-1})
L_{ele}	electric load (kWh h^{-1})
L_{EV}	charging load of BEV (kWh h^{-1})
L_{heat}	heating load (kWh h^{-1})
L_{HV}	hydrogen load of FCEV (kg h^{-1})
m_{HV}	mass of available hydrogen (kg h^{-1})
$Mean_{EV,deg}$	mean value of additional BEVs degradation caused by V2G (–)
N	number (–)
$N_{lifetime}$	lifetime of system (year)
P	power (kW)
P_y	payback period (year)
Q	energy amount (kWh)
Q_{EV}	available electricity of EV (kWh h^{-1})
Q_{pv}	power generation of PV (kWh h^{-1})
Q_{wt}	power generation of WT (kWh h^{-1})
q_{coal}	heating value of standard coal (kJ kg^{-1})
R_H	ratio of hydrogen generated from electrolysis to hydrogen demand (–)
R_{sw}	ratio of renewable electricity to total electricity (–)
$Std_{EV,deg}$	standard deviation of additional BEVs degradation caused by V2G (–)
T	temperature (K)
V	volume (m^3)
v	wind speed (m s^{-1})
$m_{H2,demand}$	mass of hydrogen consumption (kg)
$m_{H2,ELEC}$	mass of hydrogen from water electrolysis (kg)
$m_{H2,pur}$	mass of net hydrogen purchase (kg)

Greek symbols

μ	mass ratio of carbon dioxide emission from standard coal combustion (–)
λ	additional number of battery cycle due to V2G (–)
α	self-adaption factor (–)
α_1	wind shear coefficient (–)
$\eta_{c\to e}$	conversion efficiency from standard coal to electricity (%)
η_{ICE}	efficiency of ICE (%)
η_{en}	energy efficiency of V2μG network (%)
η_{ele}	electricity efficiency of V2μG network (%)
η_{WHR}	efficiency of waste heat recovery (%)

Subscripts

ava	available
bui	building
bp	backup power
comp	compressor
char	charging
disc	discharging
eg	exhaust gas
elec	electrolysis
H_2	hydrogen
hs	heat storage
jw	jacket water
m	mean
pur	purchase
res	residual
sur	surplus
t	target

1. Introduction

With the goal of Carbon Neutrality, developing low-carbon distributed energy systems has been an important strategy for all the countries, and the penetration of distributed energy systems applied in buildings has gained a large increase in recent years [1,2]. To satisfy the cooling, heating, and electric loads and reduce emissions of buildings, the distributed energy systems combining cooling, heating and power (CCHP) have attracted a lot of attention since they have relatively high energy efficiency, which is defined as the ratio of the useful energy for cooling, heating, electricity, or their combinations to the energy from the primary mover [3,4]. CCHP systems can generally convert 75–80% primary energy into the useful energy, which can be 25% more energy efficient compared to the separate heat and power systems [5]. CCHP systems normally implement internal combustion engines (ICEs) or gas turbines as the prime movers, which can be installed close to end-users with high reliability and flexibility [6,7], and they have been widely investigated in residential communities [8] and industrial park facilities [9].

With increasing demands on decarbonization, new challenges have been emerging to hinder the further developments and applications of distributed building energy systems. On the one hand, the share of renewable energy sources (RES) keeps increasing to reduce the share of fossil fuels such as natural gas or diesel used in distributed CCHP systems [10,11]. Considering the intermittency and variation of RES (e.g., solar and wind energy) [12], electric energy storage (EES) devices are required by the off-grid CCHP systems whereas the cost of EES is a big issue [13,14]. On the other hand, decarbonization in the transport sector also requires global actions, and electric vehicles (EVs) including battery electric vehicles (BEVs) and fuel cell electric vehicles (FCEVs) will be the main contributors to achieving this goal [15,16]. There are more than 10 million BEVs on the road nowadays [17,18] and the number is predicted to be over 3 billion in 2050 according to the Net Zero Emissions by 2050 scenario published by International Energy Agency (IEA) [19,20]. FCEVs have also been developing rapidly in the past few years, and over 12,900 FCEVs have been registered worldwide by the end of 2018 with a yearly increment of 80% [21]. The increasing amount of EVs will influence the design of distributed building energy systems because the charging devices located in buildings usually have higher utilization rates than charge stations, and this will bring additional energy consumption to the building energy systems [22]. Gilleran et al. [23] explored the effects of charging of EVs on the monthly electricity usage

and peak power demand of a big box store. They found that fast charging of EVs can increase the peak power demand by over 250% in some cases, and the impacts become more significant in cold-climate regions. Zhang et al. [24] demonstrated that charging of EVs could dramatically change the magnitude and shape of the future dynamic load profiles of grids under ageing transition of residents, suggesting that smart charging for the smart operation of grid and comprehensive and quantitative management of EVs development were required. Therefore, improving the stability and sustainability of building energy systems is in urgent demand.

Considering the capacity of BEVs and FCEVs in terms of electricity and hydrogen storage [25–27], they would be suitable energy carriers for the storage and transmission of renewable energy [28,54]. Thanks to the rapid development of Vehicle-to-Grid (V2G) networks, in which EVs can serve both daily cruise and energy storage functions. This has been demonstrated as an attractive and cost-efficient method [29] to improve the penetration of RES and stabilize its grid connection [30]. For the grid-connected scenario, Liu et al. [21] studied a robust energy planning approach for a hybrid PV and wind energy system in a high-rise residential building that incorporates battery and hydrogen storage technologies. The research suggested that when focusing on the supply-grid integration or supply-economy performance, the strategy which prioritizes hydrogen storage than battery storage has demonstrated wider applicability. Farahani et al. [31] presented a conceptual design for a RES energy system integrated with both BEV and FCEV. Their results showed that storage using large battery systems is more expensive than utilizing the hydrogen stored in salt caverns. The research also suggests that taking both electricity and hydrogen as energy carriers can provide a more reliable, flexible, and cheaper energy system for an office building. Liu et al. [32] developed a peer-to-peer energy trading management approach for a net-zero energy community integrated with BEV and FCEV. They found that the FCEV integrated system performs better in terms of power supply performances, and the BEV integrated system showed better performance in terms of grid integration, economic and environmental aspects. For grid-connected systems, complicated electricity trading strategies are generally required due to the power imbalance in some cases [33].

V2G service leads to the additional degradation of BEV batteries due to storing the surplus electricity of the system. Child et al. [34] studied the participation extent to a 100% RES scenario and found that high participation of V2G can efficiently decrease cost due to the small capacity required of system components. They also concluded that the additional charging and discharging processes due to V2G services will increase battery degradation and shorten battery cycle life. Bishop et al. [35] found that the battery degradation in V2G service could be minimized by reducing the battery capacity of the vehicle and restricting the number of hours connected, while the minimum impacts of providing V2G services are severe such as requiring multiple battery pack replacements over the EV lifetime. Thingvad et al. [36] gave an empirical insight into a V2G service to show the influence of V2G on battery degradation, and they found that the average usable battery capacity decreased from 23 kWh to 20.7 kWh after two years of V2G and to 18.9 kWh after five years. According to their results, two-thirds of degradation was caused by calendar ageing while one-thirds was due to charging and discharging processes. Dubarry et al. [37] studied the influence of V2G service on battery degradation and concluded that a V2G step (1 h discharging at peak demand for electricity) twice a day increased the capacity loss by 75% and the resistance by 10%. Besides, due to the uncertainty in BEV behavior, V2G services will cause uneven degradation extents among different BEVs in the V2G system [38]. Actively controlling the distribution can make V2G services fairer and meet the wishes of users.

The above references demonstrated that the presence of BEVs and FCEVs has superiority in improving the penetration of RES and stability of grid connection in distributed building energy systems, making the distributed building energy systems a promising technology to succeed in a carbon-neutrality society. However, there are still some crucial knowledge challenges in the integration of RES-based distributed energy systems and EVs. Firstly, the RES building energy systems integrated with BEVs and FCEVs are mainly discussed in the grid-connected scenario, but the off-grid scenario is also an important development trend to avoid the high cost of building a vast grid. In an off-grid scenario, there is no electricity trading between the off-grid systems and the grid, and the energy balance and operation strategy to meet the different energy loads considering the effects of EVs and V2G are still rarer. Hence, the techno-economic and environmental performance of off-grid RES building energy system with EVs need to be investigated. More importantly, V2G interactions could inevitably cause the degradation of batteries in EVs, and developing proper methods to mitigate the degradation is quite meaningful. Previous studies about the introduction of FCEVs into distributed building energy systems mainly focus on economic and power supply performances, but the potential of FCEVs in adjusting system energy distribution to minimize battery degradation of BEVs and to control the distribution of total battery degradation has not been explored and evaluated, and there is also lack of the corresponding operation strategies. Finally, the adoption of FCEVs and hydrogen as energy carriers provide a promising direction that fuel cells (FC) can be used to replace the conventional backup power equipment such as diesel engines since it is convenient to achieve the exchange and storage of hydrogen in the presence of FCEVs and backup FC, but the techno-economic performance of using ICE and FC should be comprehensively compared.

To address these challenges, this paper proposes a new concept of 'Vehicle-to-Micro-Grid (V2μG) network' that incorporates the off-grid building energy system with flexible power storage/supply provided by BEVs and FCEVs. In the proposed network, the effects of FCEV to mitigate the degradation of EV batteries caused by V2G are originally evaluated and optimized under different network scenarios with different energy management strategies. The work is conducted with three main contributions: 1) a rule-based energy management strategy is proposed to study the impact of the interaction of EVs and the V2μG network on the EV battery degradation; 2) a scenario analysis based on four working modes is conducted to evaluate the energy efficiency, costing, environmental impacts, and component ageing of the proposed V2μG network; 3) the optimum settings of system configuration, capacity, and operation strategy of the V2μG network are obtained by the NSGA-II algorithm.

The rest of this paper is organized as follows. In Section 2, an off-grid renewable building system is described, and its evaluation indicator is defined. The energy management, proposed strategy and system optimization are detailed in Section 3. In Section 4, the results and discussion on the V2μG network are presented. The main conclusions are summarized in Section 5.

2. Methods

2.1. System descriptions

As illustrated in Fig. 1, the proposed V2μG network utilizes renewable energy power generators (REPGs) as the primary mover and consists of a CCHP as the backup power supply. Two types of CCHP are studied in this paper, i.e., the CCHP powered by ICE (Fig. 1(a)) and the CCHP powered FC (Fig. 1(b)). The rest subsystems connected to the V2μG network include DC bus for charging/discharging of EVs, a hydrogen generation (HG) station with a market/trading interface, and the building power loads (e.g., electricity and heat). The wind turbine and solar PV generate electricity as the REPGs to meet eclectic loads, and the surplus renewable electricity can be stored in BEV or used by the electrolyzer and compressor for hydrogen generation. When the available power in the REPG generator cannot meet the building power demand, the backup power will provide additional electricity while recovering the waste heat from power generation and the recovered heat

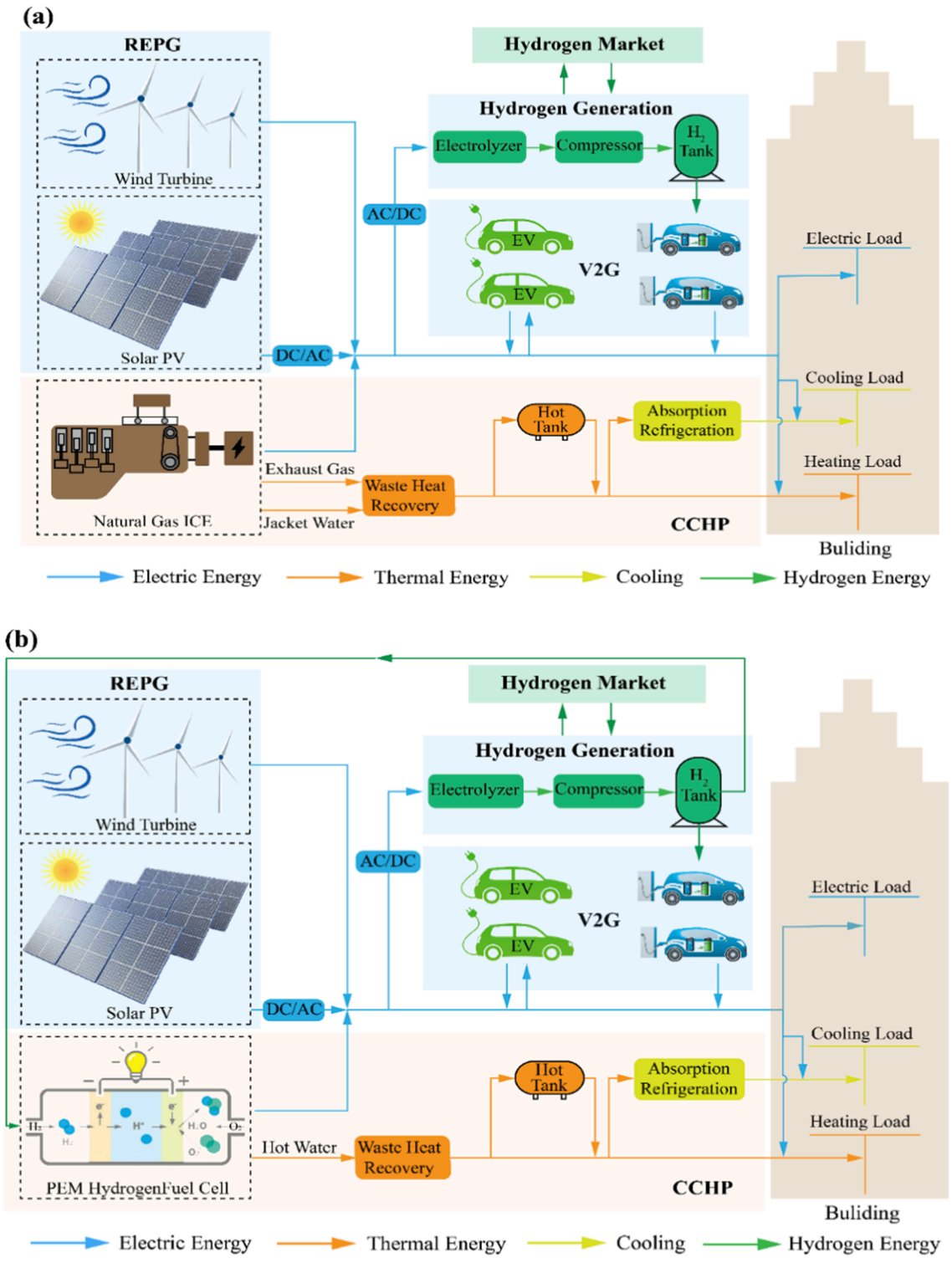

Fig. 1. The Vehicle-to-Micro-Grid (V2μG) network. (a) ICE as the backup power; (b) FC as the backup power.

will be used to meet the heating and cooling demands of the building. In the proposed network, the influence of the hydrogen market can be mitigated by adjusting the system capacity for hydrogen generation and storage. For example, in the areas that do not have the access to hydrogen markets but have high demands for hydrogen usage, the system will implement larger hydrogen tanks with higher hydrogen generation capacity so that more hydrogen can be generated and stored to fulfil the end-user demand. There are many energy transmission processes in the system and the efficiency improvement of these processes can increase power generation or power saving, which leads to better energy, economic, and environmental performances. Considering that there are many types of efficiency, and the impact on the results is relatively predictable, the common fixed values or calculation methods are taken in the manuscript, which will be detailed in section 2.2 and *Supplementary Material*. The operation strategies, e.g., how to involve EVs for better energy performance, will be detailed and discussed in section 3.

The renewable power generation (solar PV and wind turbine),

backup power generation and waste heat recovery (ICE and FC), hydrogen generation, vehicles behaviors (e.g., daily cruise mileage and schedule), weather conditions (hourly wind speed and direct normal irradiation), building information (e.g. building area and main heat transfer coefficients), and the building loads in terms of cooling, heating, and electricity are modelled using the state-of-the-art software tools (e.g., DEST, AutoCAD) based on industry data with the support from Ningbo C.S.I. Power and Machinery Group Co. Ltd. The V2G process is represented by the charging and discharging processes of the EV batteries, and the corresponding charging and discharging efficiencies decide the V2G performance. The efficiencies are taken as the common values so that we do not use the actual V2G data to validate the V2G model. On the other hand, the degradation of the battery caused by V2G is calculated based on the electric throughput of the battery, it is a common simplified method when considering battery degradation. In the research about the V2G process, many similar assumptions are used [31,32]. Considering that the purposes of the optimization are the optimal capacities of equipment and scenario selection, the main parameters of the V2μG network in this paper are listed in Table 1. It needs to be noted that the variables in Table 1 are used for the parametric analysis to explore the change rule of network performance when one factor changes. In section 4.2, all the decision variables will be optimized simultaneously to get the most suitable parameter values with specific goals. The model details can be found in the *Supplementary Material*.

In this paper, the modelling work is based on the following assumptions:

(1) The energy conversion in V2G service is mainly influenced by the charging and discharging efficiencies;
(2) There is a linear relationship between battery degradation and electricity throughput amount;
(3) Hydrogen can be sold or purchased timely;
(4) The variation of vehicle energy efficiency in different seasons is ignored;
(5) EVs joining the V2G service are considered as a part of the proposed network and the variation of the global tax ratio is ignored since most trading activities happened internally within the network.

2.2. Performance indicators of the V2μG network

2.2.1. Energy conversion efficiency

Energy efficiency can show the energy utilization ability of the V2μG network under different component capacities. The yearly energy efficiency (η_{en}) is defined as the ratio of electricity output to energy input,

$$\eta_{en} = \frac{E_{bui} + E_{EV} + E_{HFCV} + E_{H_2,out}}{Q_{solar,in} + Q_{wind,in} + Q_{H_2,in} + Q_{NG,in}} \quad (1)$$

where E_{bui} is the total electricity load of the building (including heating and cooling loads) in a year; E_{EV} is the electricity energy consumed by BEV in a year; E_{FCEV} is the electricity output of hydrogen consumed by FCEV in one year; $E_{H2,out}$ is the electricity output of surplus hydrogen in one year; and $Q_{solar,in}$, $Q_{wind,in}$, $Q_{H2,in}$, and $Q_{NG,in}$ are the energy input amounts in a year of solar, wind, hydrogen, and natural gas, respectively.

Table 1
Values of the input parameters.

Parameter	Value
Number of PV cell (N_{PV})	2000 (–)
Rated power of PV cell (P_{PV})	0.28 kW
Number of wind turbine (N_{WT})	10 (–)
Rated power of wind turbine (P_{WT})	35 kW
Power of backup power unit (P_{BP})	100 kW
Number of backup power unit (N_{BP})	3 (–)
Power of electrolyzer (P_{ELEC})	200 kW
Number of BEV (N_{EV})	150 (–)
Number of FCEV (N_{FCEV})	50 (–)

Eq. (1) mainly focuses on the energy conversion performance, and the energy with different energy levels is considered uniformly. To measure the energy conversion at the same level and reflect the electricity utilization capability of the V2μG network, the yearly electricity efficiency (η_{ele}, ratio of electricity output to input) is taken into consideration, expressed as:

$$\eta_{ele} = \frac{E_{bui} + E_{EV} + E_{HFCV} + E_{H_2,out}}{E_{solar} + E_{wind} + E_{H_2,in} + E_{NG} + E_{WHR}} \quad (2)$$

where E_{solar}, E_{wind}, $E_{H2,in}$, and E_{NG} are the electricity generated in a year by solar energy, wind energy, hydrogen via FC, natural gas via ICE, respectively; E_{WHR} is the electricity that can be saved by waste heat recovery for cooling and heating in a year. The detailed calculated methods of parameters in Eqs. (1) and (2) used for efficiency calculation are shown in the *Supplementary Material*.

2.2.2. Environmental impacts

The utilization of solar and wind energy can save a big amount of fossil fuel and reduce CO_2 emissions. To quantify the contribution of the proposed system in decarbonization, the concept of carbon dioxide reducing rate (*CDRR*) is introduced, which is defined as [39]:

$$CDRR = \mu \cdot \frac{\eta_{c\to h}^{-1} \cdot \left(E_{bui} + E_{EV} - E_{bp} + E_{H_2,ELEC}\right)}{q_{coal}} - CD_{bp} \quad (3)$$

where μ is the mass ratio of carbon dioxide emission to standard coal combustion, taken as 2.45; q_{coal} is the lower heating value of coal, given as 2.931×10^4 kJ kg^{-1}; $\eta_{c\to e}$ is the energy conversion efficiency from standard coal to electricity, taken as 40% [39]; E_{bp} is the electricity supplied by the backup power in a year; $E_{H2,ELEC}$ is the yearly electricity generated by the hydrogen from electrolysis. The first term in Eq. (3) is the carbon emission reduction due to the utilization of renewable energy rather than electricity generated from coal. CD_{bp} is the carbon dioxide that will be emitted due to the use of backup power (mainly ICE power) in one year.

The RES share (R_{sw}) is defined as the ratio of electricity from REPG to total electricity, and can reflect the degree of dependence of the V2μG network to the backup power, which is expressed as:

$$R_{sw} = \frac{E_{solar} + E_{wind} - E_{waste}}{E_{bp} + E_{solar} + E_{wind} - E_{waste}} \quad (4)$$

where E_{waste} is the renewable electricity that cannot be absorbed by the V2μG network due to limited building load and storage capacity in a year. Besides, hydrogen self-sufficiency degree (R_H) is the ratio of hydrogen generated from electrolysis of water to hydrogen demand of the V2μG network. R_H can show the dependence of the V2μG network to hydrogen market and guide for the system design in the regions with varying degrees of hydrogen market development, expressed as:

$$R_H = \frac{m_{H_2,ELEC}}{m_{H_2,demand}} \quad (5)$$

where $m_{H2,ELEC}$ and $m_{H2,demand}$ are the mass of hydrogen from water electrolysis and hydrogen consumption of the V2μG network. $m_{H2,pur}$ is the net hydrogen purchase of the V2μG network, which is the difference of $m_{H2,ELEC}$ and $m_{H2,demand}$.

2.2.3. Economy

The levelized cost of electricity (*LCOE*) is chosen as the indicator of economic performance, which is defined by:

$$LCOE = \frac{C_{total} - I_{CO_2,save}}{E_{out} \cdot N_{lifetime}} \quad (6)$$

$$E_{out} = E_{bui} + E_{EV} + E_{HFCV} + E_{H_2,out} \quad (7)$$

$$I_{CO_2,save} = CDRR \cdot CT \quad (8)$$

where $N_{lifetime}$ is the lifetime of the system, taken as 20 years, and the replacement cost of the equipment whose lifetime is shorter than 20 year is calculated. E_{out} is the electricity generation of the V2μG network in a year; $I_{CO2,save}$ is the income of CO_2 emission reduction when considering the carbon tax, and shown by Eq. (8). CT is the carbon tax and its value varies from country to country such as 13 \$ t^{-1} in Canada and 131 \$ t^{-1} in Sweden [40] in 2018. The CT of 30 \$ t^{-1} will be used as a case in this study. C_{total} is the total cost of this system,

$$C_{total} = C_{REGP} + C_{HG} + C_{CCHP} + (C_{V2G} + C_{O\&M}) \cdot \frac{(1+i)^{N_{lifetime}} - 1}{i(1+i)^{N_{lifetime}}} \quad (9)$$

where i is the interest rate, given as 10% [39]; C_{REPG}, C_{HG}, and C_{CCHP} are the investment cost of REPG, HG, and CCHP, shown as:

$$C_{REGP} = C_{PV} + C_{WT} + C_{INV} \quad (10)$$

$$C_{HG} = C_{H_2} + C_{ELEC} + C_{H_2,T} + C_{COMP} \quad (11)$$

$$C_{CCHP} = C_{NG} + C_{bp} + C_{AC} + C_{HE} + C_{Hot,T} \quad (12)$$

where C_i is the capital cost of component i; The detailed cost of components is expressed in Table 2. C_{V2G} is the additional degradation cost of V2G service, calculated as:

$$C_{V2G} = \frac{E_{V2G,EV}}{Cap_{battery} \cdot Cycle_{EV}} \cdot C_{battery} + \frac{H_{V2G,HV}}{Cycle_{HFCV}} \cdot C_{FC} \quad (13)$$

where $E_{V2G,EV}$ is the power amount of BEV discharging; $Cap_{battery}$ is the capacity of BEV; $Cycle_{EV}$ and $Cycle_{FCEV}$ are the cycle life of BEV and FCEV (shown in Table S1); $C_{battery}$ and C_{FC} are the cost of battery and FC, taken as 170 \$ kWh^{-1} and 422 \$ kW^{-1}; $H_{V2G,HV}$ is the additional working hours of FCEV caused by V2G service; $C_{O\&M}$ is the annual operation and maintenance cost of the V2μG network.

Besides *LCOE*, the payback period (P_y) can also reflect the economic performance of the network and help the decision makers evaluate the feasibility of the proposed network. The P_y is defined as:

$$P_y = \frac{C_{invest}}{E_{out} \cdot E_{price} + CT \cdot CDRR - C_{O\&M}} \quad (14)$$

where E_{price} is the electricity price of the network location, varying from 0 to 0.4 \$ kWh^{-1} around the world in 2022 [49].

Table 2
The economic parameters of the V2μG network.

Subsystem	Component	Unit cost of capital	O&M cost or ratio of capital cost
REPG	PV	995 (\$ kW^{-1}) [41]	10 (\$ kW^{-1}) [42]
	WT	1200 (\$ kW^{-1}) [42]	15 (\$ kW^{-1}) [42]
	Inverter	40 (\$ kW^{-1}) [43]	10 (\$ kW^{-1}) [43]
HG	Hydrogen cost	2.2 (\$ kg^{-1}) [44]	–
	Electrolyzer[a]	800 (\$ kW^{-1}) [44]	2% [32]
	Hydrogen tank	500 (\$ kg^{-1}) [44]	0.5% [32]
	Compressor	3900 (\$ kW^{-1}) [44]	2% [32]
CCHP	Natural gas price	0.17 (\$ kg^{-1}) [45]	–
	ICE	200 (\$ kW^{-1}) [46]	2% [47]
	FC[b]	422 (\$ kW^{-1}) [48]	2%
	Absorption chiller	200 (\$ kW^{-1}) [7]	2%
	Heat exchanger	30 (\$ kW^{-1}) [7]	2%
	Hot tank	20.1 (\$ kWh^{-1}) [39]	0.5% [39]

a: cycle life is taken as 65000 h [44], and the replacement cost is taken into consideration.
b: cycle life is taken as 5000 h, and the replacement cost is taken into consideration.

2.2.4. Battery degradation

Frequent charging and discharging will aggravate battery degradation. To exhibit the degradation of BEV caused by V2G service from the perspective of energy throughput, the concept of V2G-related equivalent battery ageing cycles, λ, is introduced as.

$$\lambda = \frac{E_{V2G,EV}}{Cap_{battery} \cdot N_{EV}} \quad (15)$$

where N_{EV} is the quantity of connected BEVs. Controlling the degradation distribution among BEVs can make the V2μG network more equitable and in line with the subjective will of different users. To show the uniformity of degradation distribution, the coefficient of variation of the degradation ($C.V_{deg}$) in this system is defined as:

$$C.V_{deg} = \frac{Std_{EV,deg}}{Mean_{EV,deg}} \quad (16)$$

where $Std_{EV,deg}$ is the standard deviation of additional BEVs degradation (expressed by additional battery cycle); $Mean_{EV,deg}$ is the mean value of additional BEVs degradation caused by V2G service.

3. Energy management and system optimization

3.1. Energy management

The novel and reference energy management strategies of scenarios are shown in Fig. 2. In Fig. 2(a), the renewable power generation, system loads, and energy storage status of the V2μG network in each hour can be obtained by the REPG and Energy Load and V2G parts. The rules of energy distribution are determined by the Operation Strategy part. In the Operation Strategy part, four scenarios are define through different combinations of the key technologies (represented by the capital letters, A, B, C, and D), i.e., (A) represents using ICE as the backup power unit, (B) represents using FC as the backup power unit, (C) represents the implementation of new energy management strategy, and (D) represents the implementation of the reference strategy. The detailed information of the four scenarios is summarized in Table 3 and principle for scenarios charging is illustrated in Fig. 2 (a). In Scenario 1(A + D): ICE is used as the backup power unit and the reference strategy is used for energy management; In Scenario 2 (B + D), FC is used as the backup power unit and the reference strategy is used for energy management; In scenario 3 (A + C), ICE is used as the backup power unit and the new energy management strategy is adopted; and in Scenario 4 (B + D), FC is used as the backup power and the new energy management strategy is chosen. The differences between the reference strategy and the new energy management strategy are compared in Fig. 2(b).

To demonstrate the energy conversion processes in the scenarios, scenario 1 is taken as an example to be explained and the differences between scenario 1 and others will be elaborated. In scenario 1, in the situation that ICE is not needed, the building and BEV loads are met by REPG. The gap between loads and RECP electricity is filled by the BEVs via storing or outputting energy. The surplus power that exceeds available BEV storage capacity in the hour is used for electrolysis. When the power of REPG and available BEV cannot meet the loads, ICE will be started to fill the gap. In the process of BEV charging and discharging, the SOC of available BEV will be sorted, and the BEV will be discharged from high to low and charged from low to high based on the SOC.

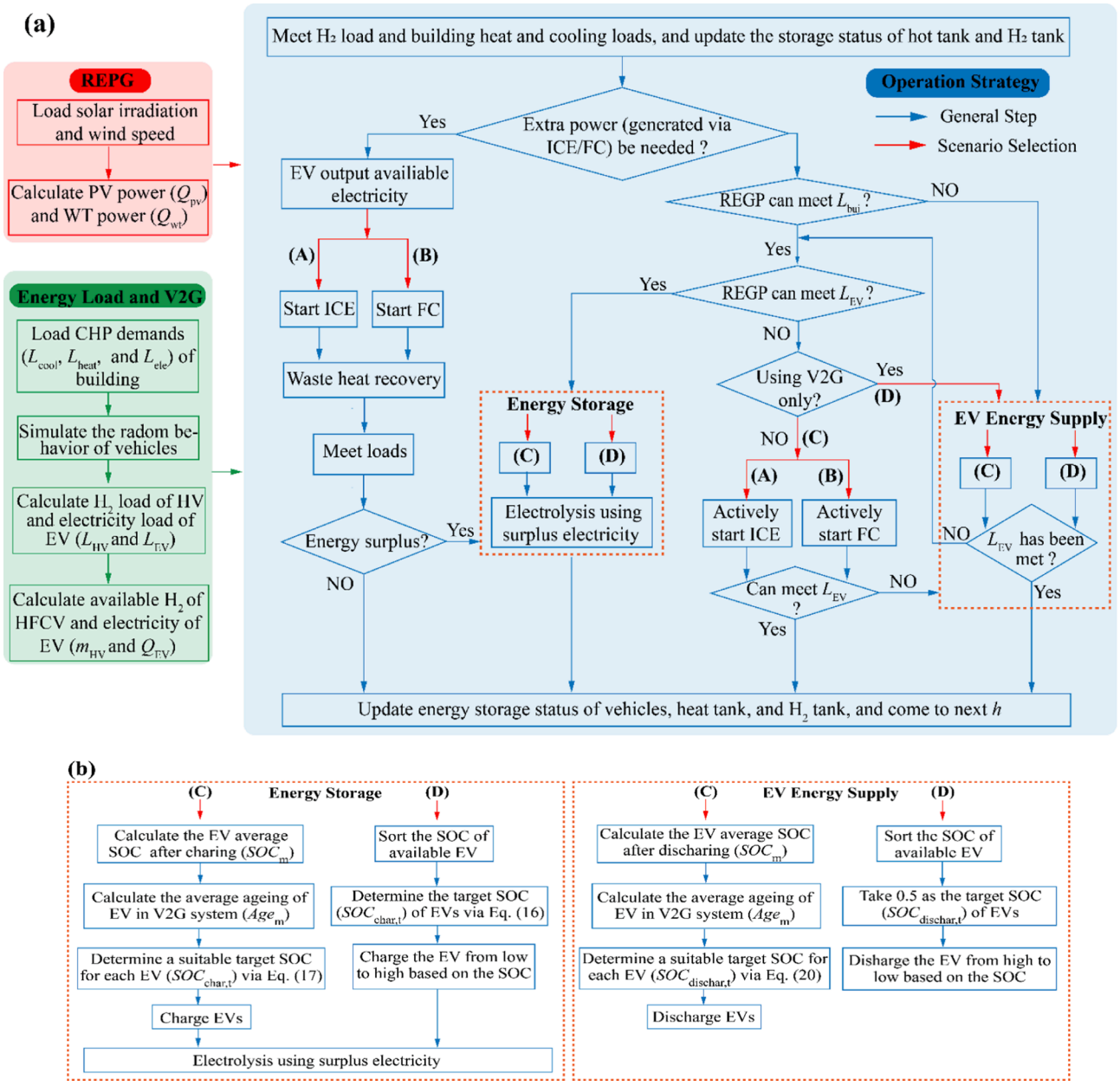

Fig. 2. The energy management strategies of the off-grid renewable energy system integrated with NEVs in different scenarios. (a) energy management strategies; (b) detailed energy storage and supply methods of novel strategy.

There are three main differences between the novel energy management and reference strategies. Firstly, from the aspect of energy storage, in the reference strategy when the SOC of BEV_i (SOC_i) is lower than 0.6, the car enters the fast charge mode and the target charge SOC of BEV_i ($SOC_{t,char,i}$) is 0.8 [45]; in other cases, the suitable SOC increment in each hour is 0.2 [45]. The target SOC is expressed as:

$$SOC_{t,char,i} = \begin{cases} 0.8 & SOC_i < 0.6 \\ SOC_i + 0.2 & 0.6 < SOC_i < 0.8 \\ 1 & SOC_i > 0.8 \end{cases} \quad (17)$$

In the novel strategy, the BEV average SOC ($SOC_{m,char}$) after the charging process and the degree of battery degradation of each BEV ($Age_{d,i}$) are considered to get the suitable target charging SOC. $SOC_{t,\,char,\,I}$ in the novel strategy can be determined by Eq. (18):

$$SOC_{t,char,i} = \begin{cases} SOC_{char,min} & SOC_{m,char} + SOC_{m,char}\cdot(1 - Age_{d,i})\cdot F < SOC_{char,min} \\ SOC_{m,char} + SOC_{m,char}\cdot(1 - Age_{d,i})\cdot F & SOC_{char,min} < SOC_{m,char} + SOC_{m,char}\cdot(1 - Age_{d,i})\cdot F < 1 \\ 1 & SOC_{m,char} + SOC_{m,char}\cdot(1 - Age_{d,i})\cdot F > 1 \end{cases} \quad (18)$$

Table 3
The description of four scenarios.

	Backup power type	Strategy type
Scenario 1 ((A)+(D))	ICE	Reference strategy
Scenario 2 ((B)+(D))	FC	Reference strategy
Scenario 3 ((A)+(C))	ICE	Novel energy management strategy
Scenario 4 ((B)+(C))	FC	Novel energy management strategy

(A): ICE as backup power; (B): FC as backup power; (C): Novel energy management strategy; (D) Reference strategy.

where $SOC_{\text{char, min}}$ is the minimum SOC for BEV storage, taken as 0.5; F is the willingness factor of the vehicle owner to the V2G service, a higher F indicates that the owner is more willing to participate in the service, and the BEV_i will have a higher $SOC_{\text{t,char,i}}$. In this research, the target is the average distribution of battery degradation so the F values of all the BEVs are taken as 1. The $SOC_{\text{m,char}}$ is calculated as:

$$SOC_{\text{m,char}} = \frac{\sum_1^{N_{\text{ava}}} SOC_\text{i} + Q_{\text{res}}}{N_{\text{ava}}} \tag{19}$$

where N_{ava} is the number of available BEV in the hour; Q_{res} is the electricity that needs to be stored; $Age_{\text{d,i}}$ can be expressed as:

$$Age_{\text{d,i}} = \frac{\lambda_\text{i}}{\lambda} \tag{20}$$

where λ_i is the degradation degree of BEV_i. However, the use of this strategy will cause a part of electricity cannot be stored by the BEV. The surplus energy will be utilized by the electrolyzer for hydrogen generation to achieve a suitable energy distribution. The $SOC_{\text{m,char}}$ in Eq. (18) can reduce the flow of electricity among BEVs, causing a decrease in battery degradation. $Age_{\text{d,i}}$ will make the degradation fairer and more desirable for the BEV owner.

The second difference is the different BEV power supply methods. In the reference strategy, the target SOC in the discharging process ($SOC_{\text{t,disc,i}}$) is 0.5 [50]. In the novel strategy, similar to the charging process, the $SOC_{\text{t,disc,i}}$ includes the influences of the mean SOC after discharging ($SOC_{\text{m,disc}}$), $Age_{\text{d,i}}$, self-adaption factor (α, to ensure enough energy can be output), and the willing of owners on the V2G service ($1/F$), which can be expressed as:

$$SOC_{\text{t,disc,i}} = \begin{cases} SOC_{\text{disc,min}} & SOC_{\text{m,disc}} \cdot Age_{\text{d,i}} \cdot \dfrac{\alpha}{F} < SOC_{\text{disc,min}} \\ SOC_{\text{m,disc}} \cdot Age_{\text{d,i}} \cdot \dfrac{\alpha}{F} & SOC_{\text{disc,min}} < SOC_{\text{m,disc}} \cdot Age_{\text{d,i}} \cdot \dfrac{\alpha}{F} < 1 \\ 1 & SOC_{\text{m,disc}} \cdot Age_{\text{d,i}} \cdot \dfrac{\alpha}{F} > 1 \end{cases} \tag{21}$$

where $SOC_{\text{disc,min}}$ is the lower limit of BEV discharging, taken as 0.5; α is the self-adaption factor, taken as 1 firstly, and if the electricity requirement cannot be satisfied, α will decrease and the BEV will continually discharge until meeting the gap; F is the willing factor of the EV owners on the V2G service. $1/F$ can adjust the degree of participation of different users. $SOC_{\text{m,disc}}$ is shown as:

$$SOC_{\text{m,char}} = \frac{\sum_1^{N_{\text{ava}}} SOC_\text{i} - Q_{\text{gap}}}{N_{\text{ava}}} \tag{22}$$

where Q_{gap} is the electricity gap that needs to be met by BEV.

The strategy improvement in charging and discharging allows the SOC of vehicles to be closer after charging, reducing the unnecessary flow of energy between vehicles and thus reducing the degradation of battery. Besides, the electricity share from vehicles that has less degradation and more willing in V2G service is improved, which can control the distribution of degradation among BEVs.

Thirdly, when a part of the EVs with surplus electricity needs to satisfy the BEV load that cannot be met by the REPG, the reference strategy sorts the SOC of BEV and discharges the BEV from high to low based on the SOC. In the novel strategy, when the BEV load is bigger than the minimum starting load of backup power, the backup power will be actively started to meet the BEV load, and if the load still cannot be met, the BEV will supply the required power. This operation makes the energy that would otherwise flow between BEVs can be used for daily cruises. Meanwhile, compared to that in reference, the BEV load after this operation in the novel strategy will be smaller in the next few hours, so the V2μG network needs for ICE will not significantly increase. It needs to be noted that the active start of the backup power is to use backup power at a more suitable time (rather than when the V2μG network has an energy gap) to reduce the transmission of electricity between BEVs.

3.2. System optimization

NSGA-II with fast calculation speed and strong robustness is utilized to optimize the V2μG network with the objective of the highest *CDRR* and minimum *LCOE* (detailed in section 4.2) via Python software. Systems with energy gaps at any time of the year will be discarded. The mathematic model of the V2μG network design can be expressed as:

$$\left[N_{\text{PV}}^*,\ N_{\text{WT}}^*,\ P_{\text{BP}}^*,\ P_{\text{ELEC}}^*,\ S^*\right] = \arg\min\left(-CDRR, LCOE\right) \quad \text{s.t.} \begin{cases} N_{\text{PV}} \in \{1,2,3,\ldots,5000\} \\ N_{\text{WT}} \in \{1,2,3,\ldots,30\} \\ P_{\text{BP}} \in \{50,51,52\ldots,150\} \\ P_{\text{ELEC}} \in \{1,2,3\ldots,600\} \\ S \in \{1,2,3,4\} \end{cases} \tag{23}$$

where * represents the optimal value of each decision variable. The specifications of the optimization algorithm are listed in Table 4. To balance the calculation efficiency and accuracy, the number of generations and population size are taken as 50 and 600. The crossover fraction of 0.9 and mutation probability of 0.1 are common values in genetic algorithms. The ranges of decision variables are decided based on a parametric analysis which will be shown in section 4.1. The program flow chart of the optimization is shown in Fig. 3. The time interval in this research is one hour. Notably, in addition to the usual capacity optimization, the scenario selection which can also influence the performance of the V2μG network is treated as a decision variable and optimized simultaneously.

To evaluate the performance of the algorithm and the optimization result [51], two common performance indicators of multi-objective optimization, Hypervolume (*HV*) and *Spacing* are used. *HV* represents the volume of the region in the target space surrounded by the reference points and the non-dominated solution set obtained by the algorithm, which reflects the overall performance of the algorithm. *Spacing* is the standard deviation of the minimum distance from each solution to the other solution and can estimate the diversity for the achieved Pareto

Table 4
Specifications of the optimization algorithm.

Parameter	Value
Mathematical algorithm	NSGA-II
Number of generations	50
Target dimension	2
Population size	600
Number of decision variables	5
Crossover fraction	0.9
Mutation probability	0.1
Number of PV cell (–)	1–5000
Number of wind turbine (–)	1–30
Power of backup power unit (kW)	50–150
Power of electrolyzer (kW)	1–600
Scenario selection (–)	1–4

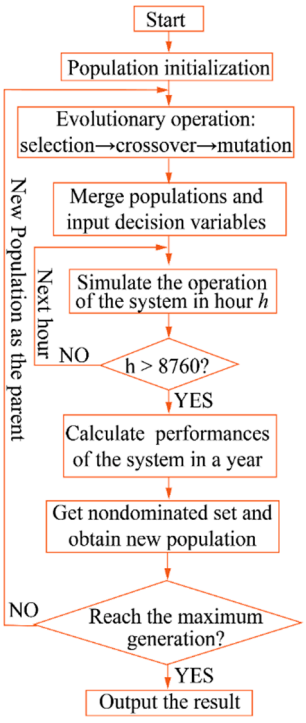

Fig. 3. Program flow chart of the optimization.

Front. They can be expressed as:

$$HV = \delta\left(\bigcup_{i=1}^{n} v_i\right) \tag{24}$$

$$Spacing = \sqrt{\frac{1}{n-1}\sum_{i=1}^{n}(\bar{d} - d_i)^2} \tag{25}$$

where δ is the Lebesgue measure; n is the number of non-dominant solutions; v_i is hypervolume of the reference point and the solution i in the solution set. Further details about these indicators can be found in [52].

4. Results and discussion

In this section, the results of the parametric analysis are illustrated. The crucial parameters and scenario selection are optimized simultaneously with multiple objectives to get the optimal system. Then the results of optimal system performance analyses are shown. The basic values of crucial parameters in the parametric analysis have been listed in Table 1. The calculations are based on the weather conditions in Beijing city, and the weather conditions are introduced in the *Supplementary Material*.

4.1. Parametric analysis

4.1.1. Number of solar PV cells

Solar PV and wind turbines are the main power generation equipment of the V2μG network. Fig. 4 shows the V2μG network performances with different numbers of solar PV. In Fig. 4(a), η_{en}, *CDRR*, and *LCOE* are

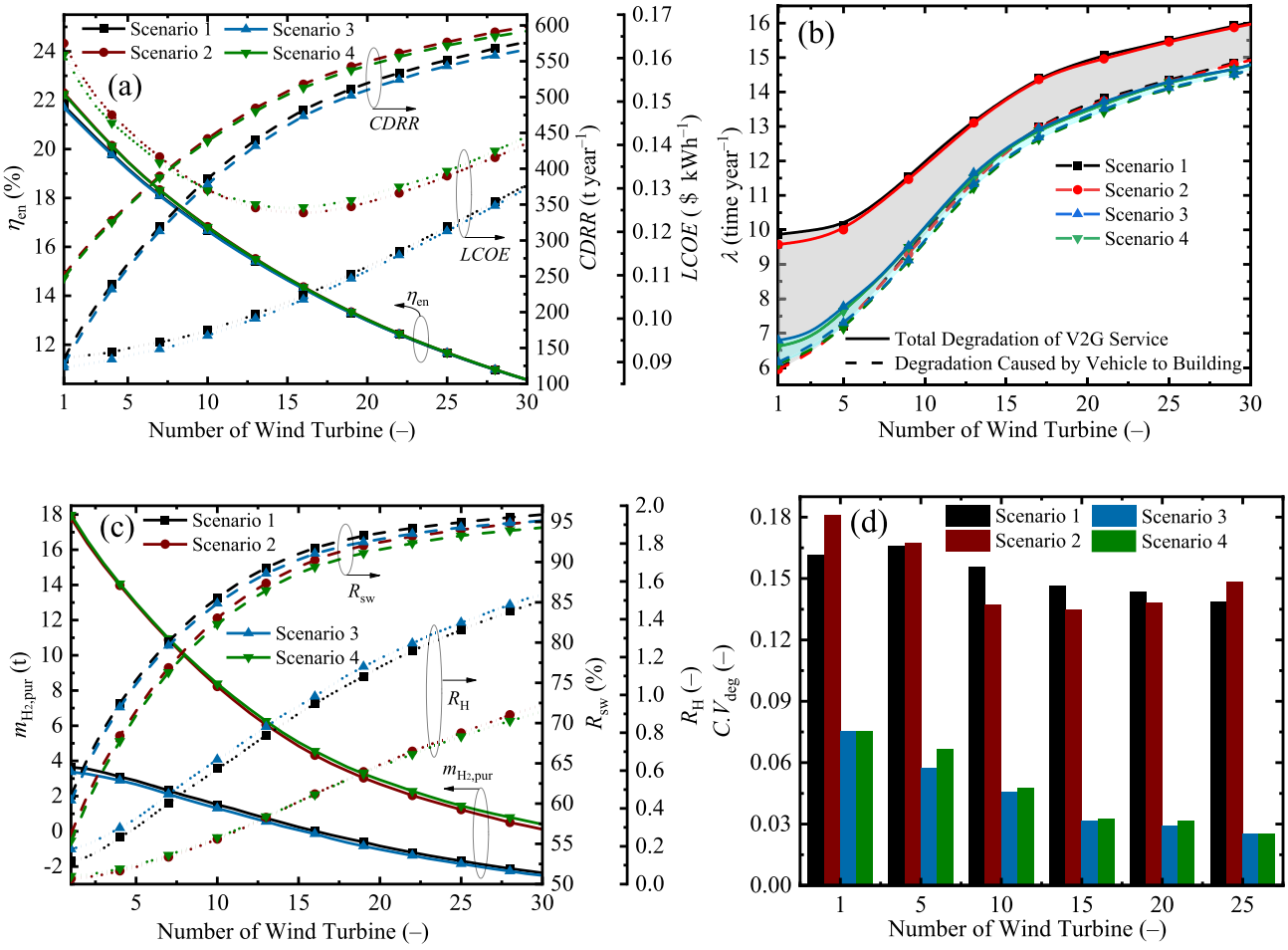

Fig. 4. System performances in different numbers of solar PV cells. (a) η_{en}, *CDRR*, and *LCOE*; (b) total degradation of V2G service and degradation caused by vehicle to the building; (c) $m_{H2,pur}$, R_{sw}, and R_H; (d) $C.V_{deg}$.

exhibited. With the N_{PV} increasing, η_{en} decreases mainly because the energy generated at the solar rich time cannot be fully used by the V2μG network. The η_{en} is also influenced by the type and electricity generation share of backup power. In the proposed V2μG network, the share of electricity generated from backup power is relatively small, and by introducing waste heat recovery, the difference between ICEs and FCs is narrowed. This is because the heat quality of the ICE is better than FC so that more high grade heat can be recovered from the ICE and thus can save more electricity for heating and cooling. High N_{PV} means that more solar energy can be directly utilized or converted into hydrogen, and thus the *CDRR* is high. The *CDRRs* of scenarios 2 and 4 are higher than that of scenarios 1 and 3 due to the CO_2 emission caused by ICEs. With the same backup power type, the *CDRR* of scenarios 3 and 4 are slightly smaller than that of scenarios 1 and 2, in which the N_{PV} is about 1500. The reason is that actively starting backup power in scenarios 3 and 4 will increase the overall SOC of BEV which slightly decreases the system's energy storage capability and thus leads to less solar energy utilization and *CDRR*. The *LCOEs* of scenarios 1 and 3 are lower than that of scenarios 2 and 4 due to the cheaper price of purchasing ICEs. With the increase of N_{PV}, the V2μG network load is constant, and the utilization rate of each PV cell decreases so the *LCOE* will increase. In scenarios 2 and 4, the cycle life of FC is 5000 h and the increase of N_{PV} can decrease the working hour and the replacement cost of FC, which decreases the *LCOE* of scenarios. Thus, there are minimum *LCOE* in scenarios 2 and 4 at an N_{PV} of about 2000.

Fig. 4(b) shows the degradation of the battery in the EVs that are connected to the V2μG network. The degradation contains the degradation caused by the electricity supply for buildings and the electricity transmission from vehicle to vehicle. The latter can be reduced by the reasonable distribution of power when charging or discharging the BEVs, and it is represented by the colored area between the solid line and the corresponding dotted line in Fig. 4(b). The choice of charge and discharge strategy, rather than the type of backup power, is the main factor that influences the degradation of BEVs. The colored areas of scenarios 3 and 4 are significantly smaller than that of scenarios 1 and 2, indicating that a lot of meaningless power exchange between vehicles is avoided and the degradation is reduced. This improvement is achieved by considering the average SOC of BEVs after charging or discharging, and then getting the suitable SOC for each vehicle based on its own SOC and the V2μG network expected average SOC (Eqs. (18) and (21)). Thus, the SOC of BEVs will be closer to each other than the reference strategy, and the requirement to transfer electricity between vehicles can be reduced.

The $m_{H2,pur}$, R_{sw}, and R_H are exhibited in Fig. 4(c). As the increase of N_{PV}, more PV electricity will be generated and used to electrolyze water, so the R_{sw} increases and $m_{H2,pur}$ decreases. The hydrogen demand decreases due to more hydrogen generation, and thus the R_H goes up. In scenarios 1 and 3, hydrogen will not be consumed by the backup power so the $m_{H2,pur}$ is smaller, and the R_H is bigger than those in scenarios 2 and 4. At high N_{PV}, the $m_{H2,pur}$ is negative, indicating the V2μG network provides a net export of hydrogen. The R_{sw} of scenarios 1 and 3 are higher than that of scenarios 2 and 4. The reason is that ICE has the waste heat with a higher energy grade and can meet more cooling demand than that of FC, and thus the required amount of backup power is smaller, which decreases the denominator of R_{sw} (Eq. (4)).

To show the degradation distribution among BEVs, $C.V_{deg}$ is shown

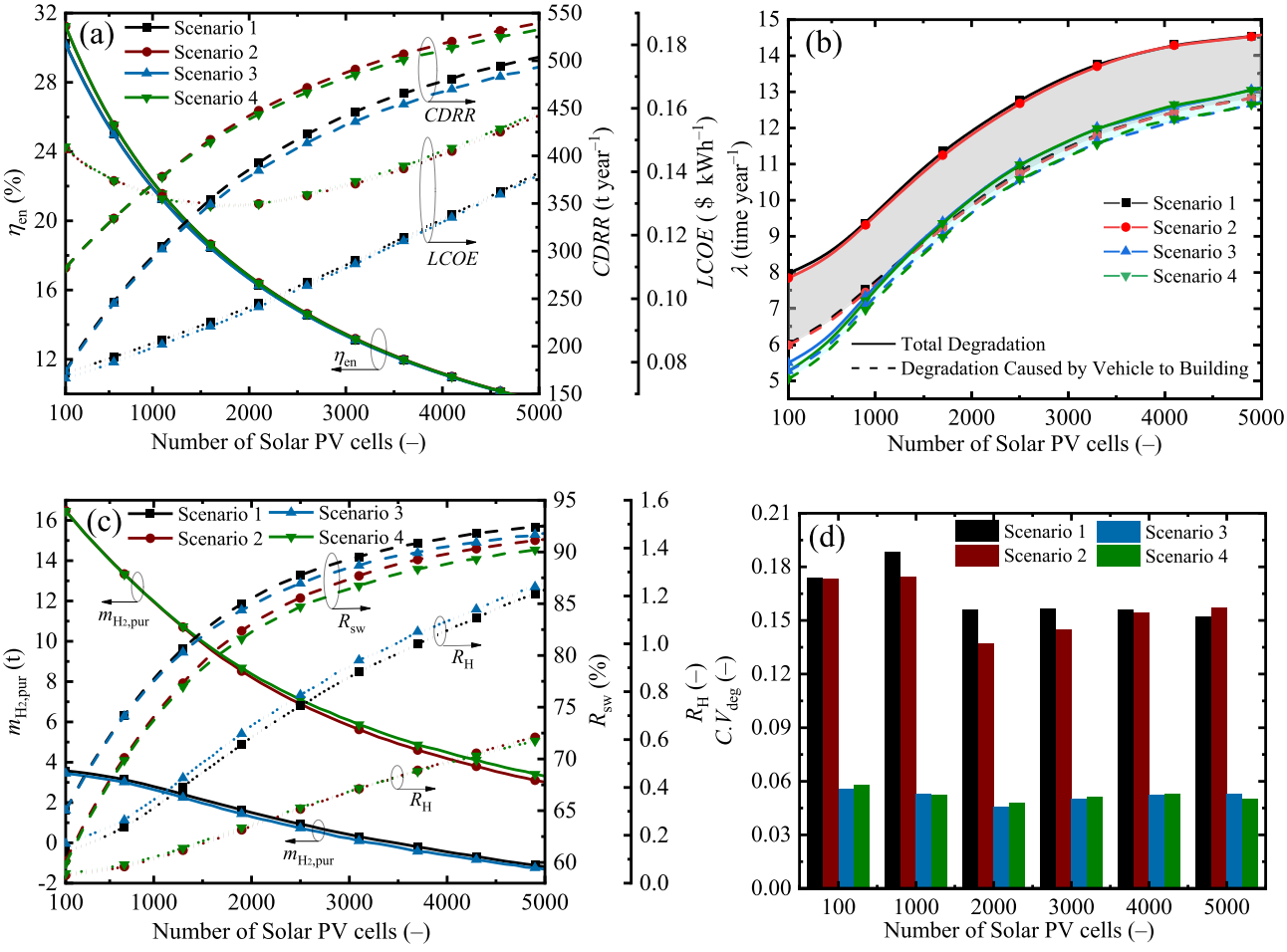

Fig. 5. System performances in different numbers of wind turbines. (a) η_{en}, *CDRR*, and *LCOE*; (b) λ; (c) Weight of purchased hydrogen ($m_{H2,pur}$), R_{sw}, and R_H; (d) $C.V_{deg}$.

in Fig. 4(d). In the absence of significant deterioration in other indicators (Fig. 4(a) and (c)), using the novel energy management strategy can significantly decrease the $C.V_{deg}$, indicating that the distribution of degradation becomes more uniform. The results are achieved by considering the degradation degree of each BEV when charging and discharging and then obtaining the target SOC based on the degradation of each BEV. As discussed in section 3, the introduction of F can make the strategy suitable for different target SOC requirements of different users, and it is not limited to making the degradation distribution among BEVs uniform.

4.1.2. Number of wind turbines

The V2μG network performances in different numbers of wind turbines are shown in Fig. 5. The influence of N_{WT} is similar to that of N_{PV} while some differences should be noted. Firstly, at small N_{WT} (e.g., 1) in Fig. 5(a), the η_{en} is much smaller than that at small N_{PV} in Fig. 4. The reason is that small N_{WT} means the renewable electricity is mainly generated by the PV which has a lower generating efficiency than that of WT (based on Eqs. (S1) and (S3)), so the η_{en} is small. Secondly, in Fig. 5 (d), the $C.V_{deg}$ of scenarios 3 and 4 decreases with the N_{WT} increasing, while that in Fig. 4(d) has little change with the increase of N_{PV}. This is because solar power is the main energy source at small N_{WT}, and the solar rich time is usually at daylight when the amount of available vehicles in the community is little. In all the scenarios, if the available battery storage is small such as at noon, the first thing is to store all the electricity rather than to get a better distribution. On the contrary, the wind-rich time like in the wee hours usually has more available vehicles, which means there is relatively enough battery storage room to achieve the adjustment on the distribution via the novel strategy in scenarios 3 and 4. Thus, as the increase of N_{WT}, the $C.V_{deg}$ decreases.

4.1.3. Rated power of ICE/FC

Backup power can ensure the stable operation of the V2μG network, and Fig. 6 shows the V2μG network performances in different rated powers of ICE/FC. The rated power of ICE/FC will not significantly change the electricity generation share of backup power, and thus it will not influence the η_{en} which is not shown in Fig. 6. With the increase in rated power, the capital cost of the V2μG network increases, causing an increase in *LCOE* (Fig. 6(a)). A higher rated power will lead to more additional power generation and fuel consumption when the power requirement is smaller than the start power. Therefore, the *CDRR* in scenarios 1 and 3 (Fig. 6(a)) slightly decreases, and the degradation of the battery (Fig. 6(b)) increases a little. In Fig. 6(c), the change of rated power will not influence the regulating effect in scenarios 3 and 4 on the distribution of degradation. It can be seen in Fig. 6 that the increases in the rated power of ICE/FC have negative influences on the V2μG network performance. A too-small rated power (e.g., 10 kW) cannot maintain the stable operation of the V2μG network. Thus, the rated power of ICE/FC also needs to be optimized.

4.1.4. Rated power of electrolyzer

The electrolyzer can use the excess electricity in this system after storing it in BEVs. Thus it only decides the ratio of electricity used for electrolysis and wasted electricity, and will not influence the $C.V_{deg}$. The

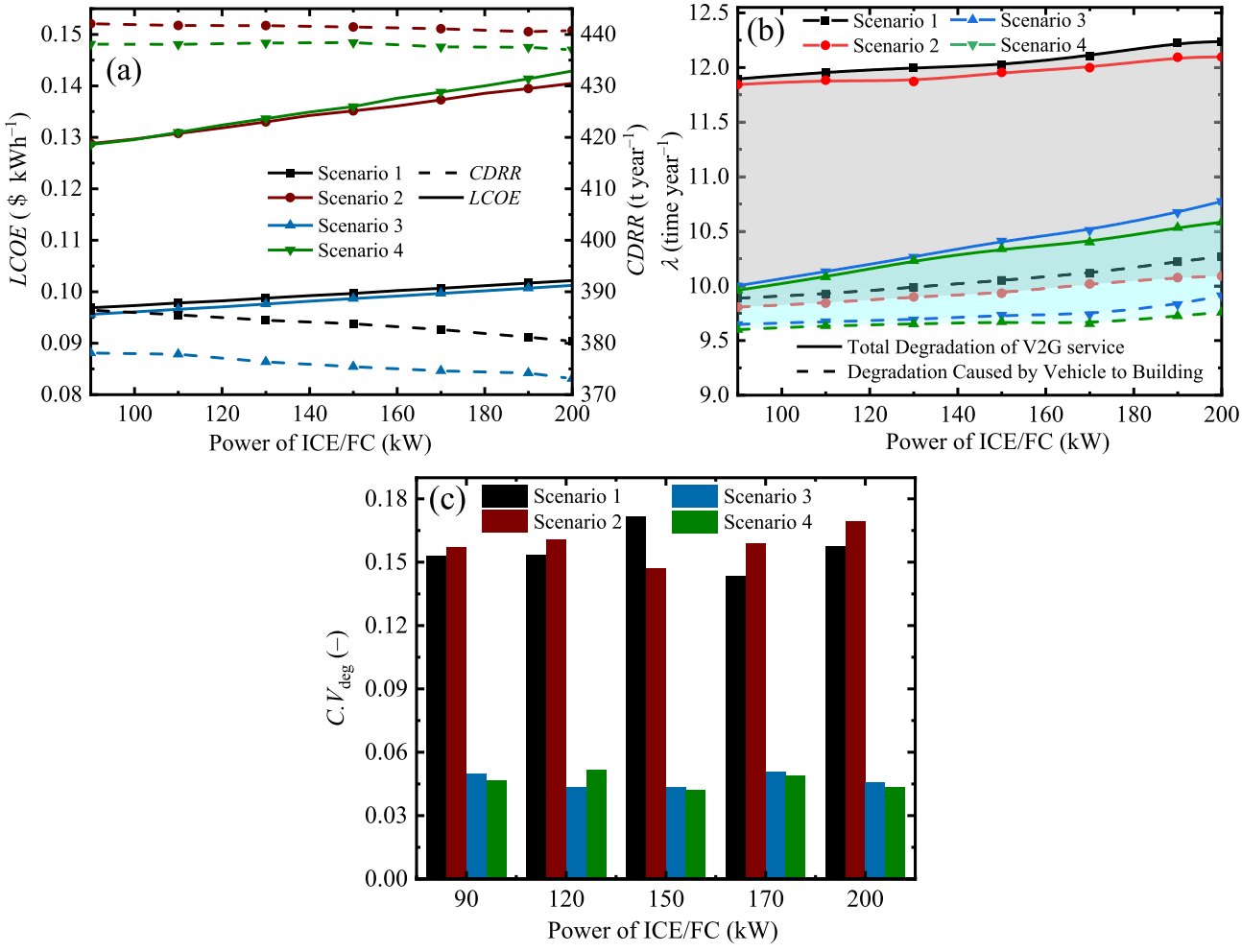

Fig. 6. System performances in different rated power of ICE/FC. (a) *CDRR*, and *LCOE*; (b) λ; (c) $C.V_{deg}$.

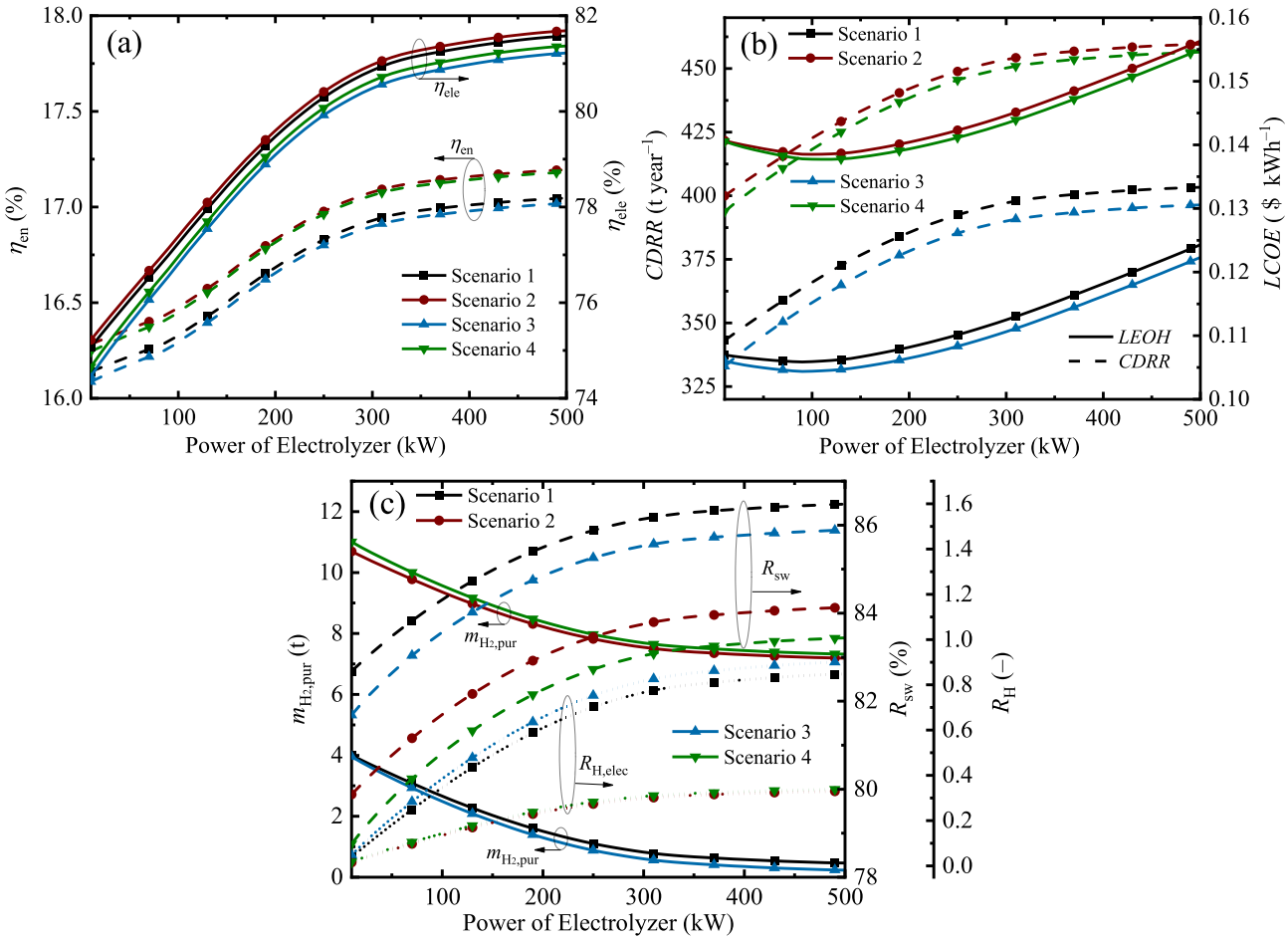

Fig. 7. System performances in different rated power of electrolyzer. (a) η_{en} and η_{ele}; (b) *CDRR* and *LCOE*; (c) $m_{H2,pur}$, R_{sw}, and R_H.

portion of power that exceeds the rated power of the electrolyzer is wasted. Thus, the rated power of the electrolyzer will influence the V2μG network performances, and the results in different rated power of the electrolyzer are shown in Fig. 7. In Fig. 7(a), as the electrolyzer rated power increases, the η_{en} and η_{ele} increase because more renewable electricity that cannot be stored in the BEVs is converted into hydrogen. Meanwhile, the *CDRR* in Fig. 7(b), $R_{sw,}$ and R_H in Fig. 7(c) also go up due to more hydrogen generation and RES utilization. At the high rated power of the electrolyzer such as 500 kW, growth in these indicators is flattening out because the electrolyzer can only use the excess energy which is limited by the rated power of WT and PV. In Fig. 7(b), the electrolyser has optimal rated power to get the minimum *LCOE* in scenarios. The reason is that the increase in the rated power of the electrolyzer (e.g., 50 kW) will generate more electricity for the V2μG network, while a too big rated power of the electrolyzer will lead to a high capital and replacement cost.

As shown in Figs. 4–7, scenarios have some differences in system performances. In the choice of backup power type, scenarios 1 and 3 get a lower *CDRR* than that of scenarios 2 and 4 due to the CO_2 emission of natural gas utilization, while the cost of scenarios 1 and 3 is notably lower than that of scenarios 2 and 4 because of the usage of relatively cheap ICE. From the perspective of energy management strategy, using the novel strategy in scenarios 3 and 4 leads to a slight disadvantage in *CDRR* because the relatively high system average SOC caused by the active start of backup power will give rise to some waste of renewable electricity. On the other hand, using the novel strategy can significantly reduce the total degradation of the V2μG network and get a more evenly distribution of degradation. Scenario 3 has the minimum *LCOE* due to the relatively cheap ICE and the low degradation cost (calculated by Eq. (13)). Based on the above discussion, the scenarios, N_{PV}, N_{WT}, rated powers of ICE/FC and electrolyzer, influence the V2μG network performances simultaneously, which need to be optimized to get the optimal system.

4.2. Optimization and optimal system analysis

Considering that the capacity parameters and scenarios discussed in section 4.1 can affect the performance of the V2μG network, synchronous optimization of them is necessary to get the optimal system. Based on the results of parametric analysis, a change in any one of the decision variables will affect *LCOE* and *CDRR*. Besides, as the cost performance of the V2μG network (the best in four scenarios) improves, so does the degradation and energy efficiency performances, while the *CDRR* deteriorates. Therefore, in this section, the highest *CDRR* and minimum *LCOE* are chosen as two objectives for optimization via the NSGA-II algorithm. A multi-objective optimization algorithm is used in this research to determine the optimal solution based on 20 individual trials. Fig. 8 shows the optimization and algorithm performance evaluation results. In the frontier of Fig. 8(a), if the *LCOE* needs to be further decreased, the *CDRR* performance must be sacrificed. Each point in the frontier represents a kind of system capacity and scenario selection. The highest *CDRR* and lowest *LCOE* can be 834.14 t year^{-1} and 0.054 $ kWh^{-1}, which cannot be obtained simultaneously. The *HV* and *Spacing* are exhibited in Fig. 8(b). As the increase of generation, the *HV* goes up and the *Spacing* decreases, showing the performance improvement of the algorithm. The Pareto frontier contains many optimum points for the multiple objectives. The Technique for Order of Preference by Similarity to Ideal Solution (TOPSIS) is a multi-criteria decision analysis method

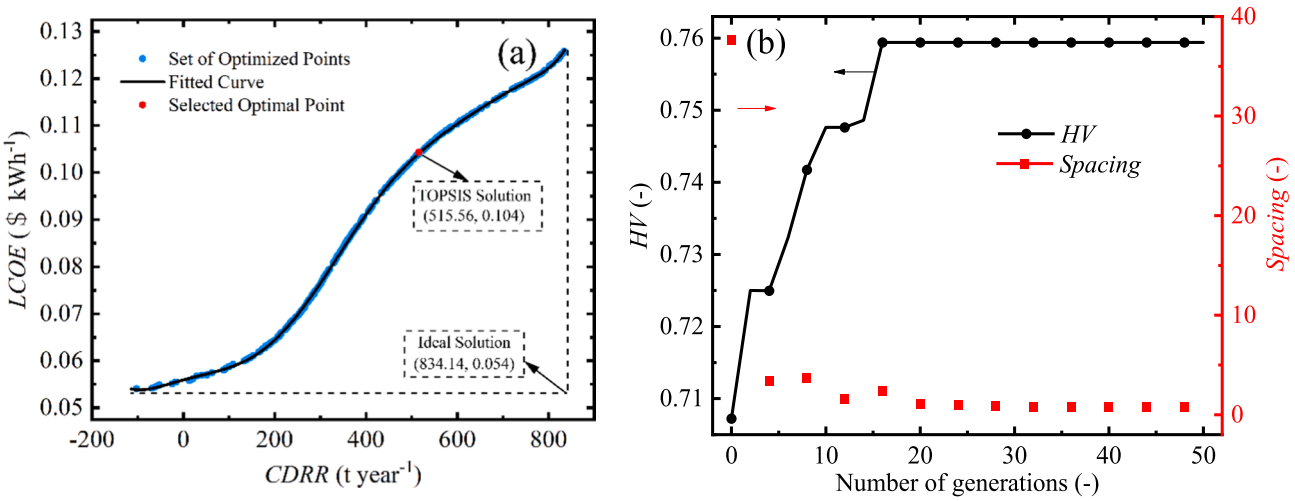

Fig. 8. Optimization and algorithm performance evaluation results. (a) Pareto frontier of the V2μG network with the objective of the highest *CDRR* and minimum *LCOE*; (b) *HV* and *Spacing* at different numbers of generations.

Table 5
The parameters of the selected optimal point.

CDRR (t year^{-1})	*LCOE* ($ kWh^{-1})	N_{PV} (–)	N_{WT} (–)	Rated power of ICE (kW)	Rated power of electrolyzer (kW)	Scenario (–)
515.56	0.104	1954	18	70	278	3

and it is used to select the suitable point for further analysis of the optimized V2μG network. An optimal point whose *CDRR* and *LCOE* are 515.56 t year^{-1} and 0.104 $ kWh^{-1} is chosen as a case based on the TOPSIS method [53]. The corresponding parameters of this optimal point are shown in Table 5.

To exhibit the energy conversion processes and corresponding energy loss of the optimal system, Fig. 9 shows the annual energy flow of the V2μG network. The percentages of different electricity usage in Fig. 9 are based on the available amount of electricity, and other forms of energy only show the amount. ICE as the backup power just needs to supply 6.2% electricity, indicating the high share of renewable energy in the proposed V2μG network. Meanwhile, the waste heat of ICE can meet a 57.6 MWh heating load and 10.3 MWh cooling load of the building. Due to the intermittency of RES and the uncertain behavior of vehicles, about 29.3% of electricity cannot be directly utilized by building or stored in BEVs and is used to electrolyze water. About 20.8% of electricity is converted into the chemical energy of hydrogen, and the V2μG network has an annual surplus of 2495.5 kg of hydrogen, which will be sold to the market. In an ideal scenario, i.e. the network has an infinite

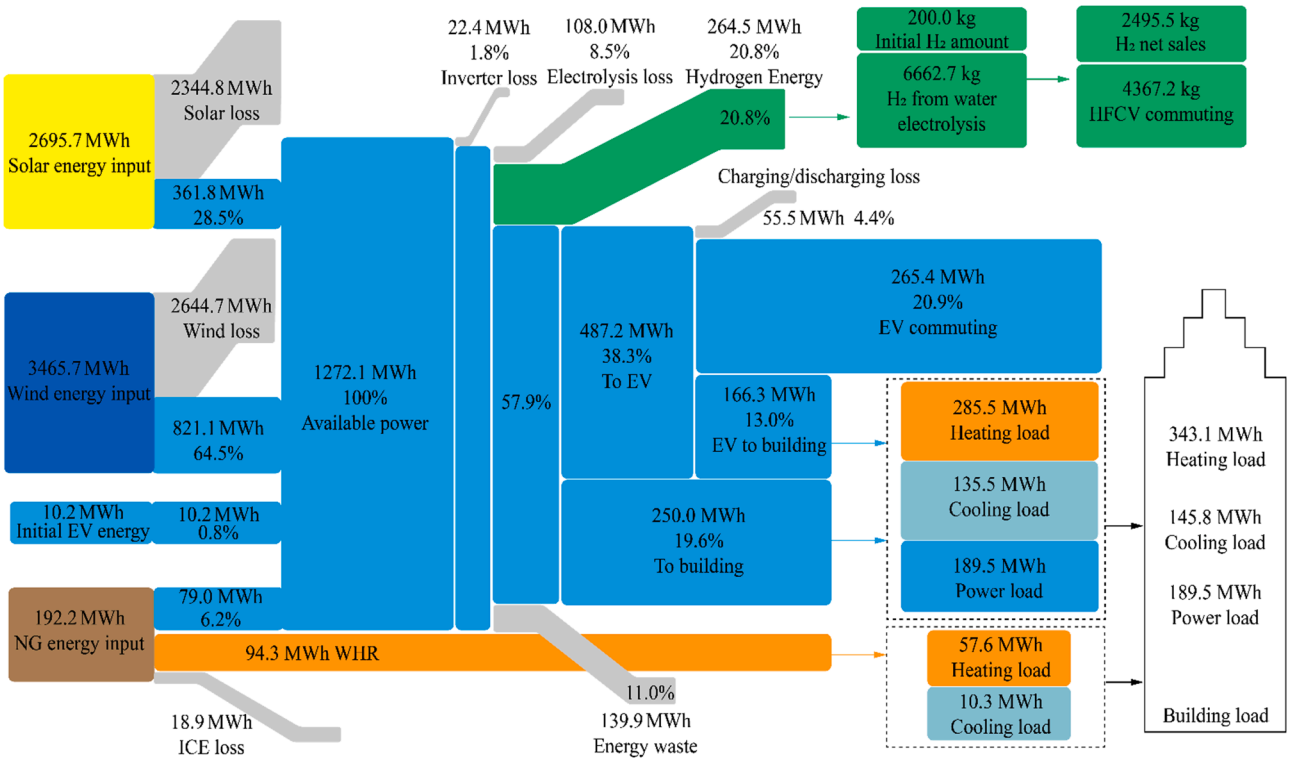

Fig. 9. The annual energy flow of the optimal system.

number of EVs and FCEVs, all the energy will be stored and there would be no wasted energy. However, the proposed network (as illustrated in Fig. 9) is optimized for the objectives of *LCOE* and *CDRR*, therefore, the cost of the network restricts the increase of the electrolyzer's rated power and the electricity storage capacity of FCEVs. Thus, there is still 11.0% of electricity, the biggest electricity loss in the energy conversion process, wasted because of the limited battery capacity of BEVs and rated power of electrolyzer. V2G service makes the system's power usage more flexible, and 13% of electricity is stored in the BEV first and then supplied to the building.

The V2μG network power balances in typical days of four quarters over a year in Beijing are shown in Fig. 10 to exhibit the different working statuses of the optimized system. In Fig. 10(a), wind energy is the main energy source during the day, and the loads are small in the afternoon, leading to lots of BEV electricity storage. Between 18 and 22o'clock, the BEV will discharge some power to meet the building load due to the lack of RES. Fig. 10(b) represents a day in the second quarter without heating or cooling load, the PV power is abundant on this day and the average SOC of available BEVs is at a relatively high level, and thus a big part of power is used by electrolysis. On the day of the third quarter (Fig. 10(c)), the cooling load is strong, and the surplus power after meeting the load is stored or used to electrolyze. At about 19–23o'clock, there is a lot of BEV discharge to meet the relatively big requirement of cooling. Fig. 10(d) shows a day in the fourth quarter that lacks RES and has a relatively low average SOC of available BEVs. ICE becomes the essential equipment to maintain the V2μG network operation in this situation, which works 15 h in the day to meet loads. The results of Fig. 10 show the diversity of energy supply and the stability of operation of the optimized system under different weather and building loads.

Fig. 11 exhibits the cost proportion of the optimized system. Notably, the yearly battery degradation cost of the V2G service is categorized into O&M cost due to the similar calculation method (Eq. (9)) and billing cycle. The REPG part accounts for 62.61% of the V2μG network cost. For the CCHP, absorption chiller, natural gas, and ICE are the main cost, taking the share of 2.71%, 2.12%, and 1.92%, respectively. Electrolyzer (11.81% of the total system cost) is the primary cost in the HG part, and the hydrogen cost of the optimized system is −4.96% due to the net sale of hydrogen in a year (shown in Fig. 9). 6.83% of the cost is generated due to the degradation of the V2G service, and the O&M cost of other equipment accounts for 10.92%. The results of Fig. 11 can guide the suitable adjustment of the V2μG network to different *LCOE* targets.

To evaluate the feasibility of the proposed network, the payback period of the network under different electricity prices and carbon taxes is shown in Fig. 12. In the region with high electricity prices (e.g., Germany) and high carbon tax (e.g., Sweden), the proposed network has more promising application prospects due to its electricity generation and carbon reduction. The payback period of the network can be about 8 years with an electricity price of 0.3 \$ kWh^{-1} and a carbon tax of 10 \$ t^{-1}.

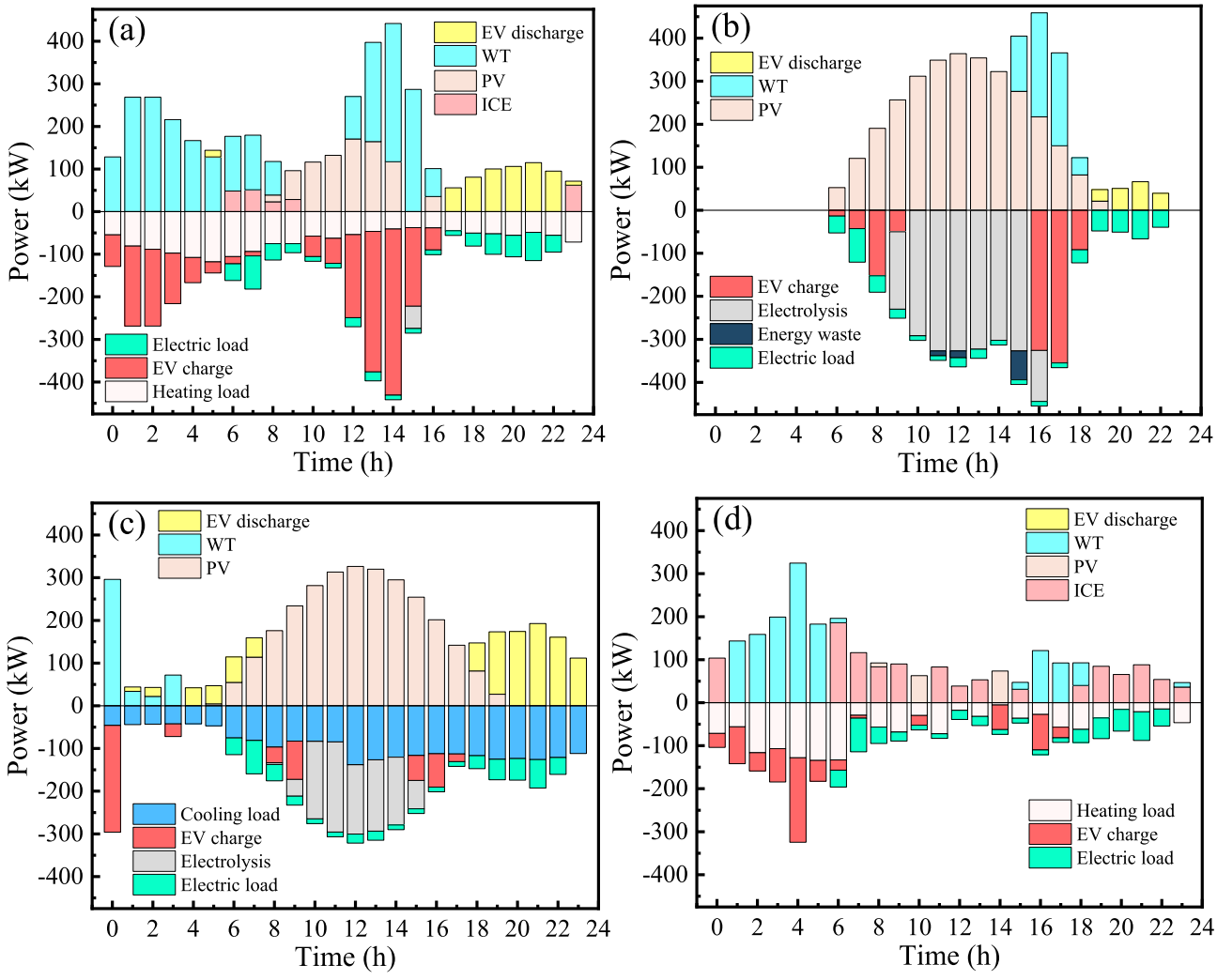

Fig. 10. Power balances of the optimized system in typical days of four quarters in a year in Beijing. (a) the first quarter (January 6th as a case), (b) the second quarter (May 19th) (c) the third quarter (July 7th as a case), and (d) the fourth quarter (December 26th).

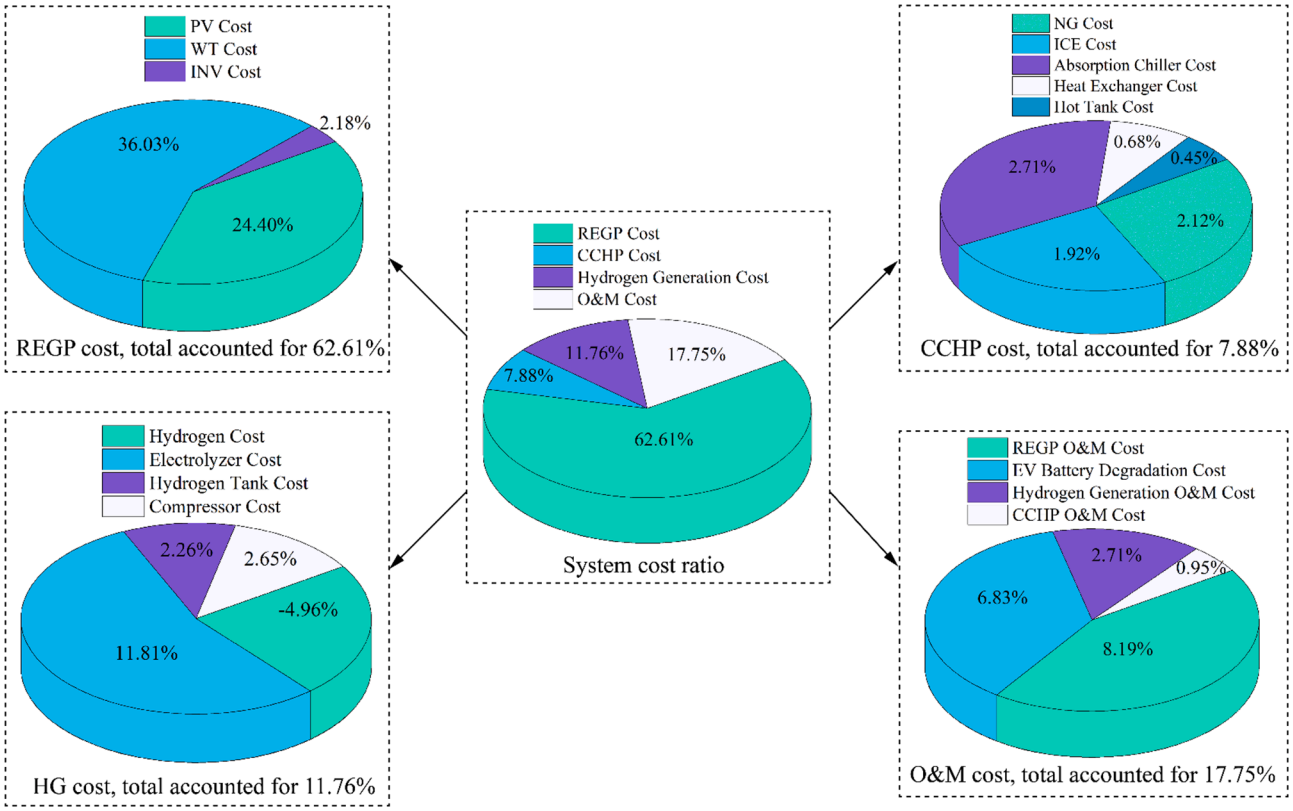

Fig. 11. Cost ratio of the main part of the optimal system.

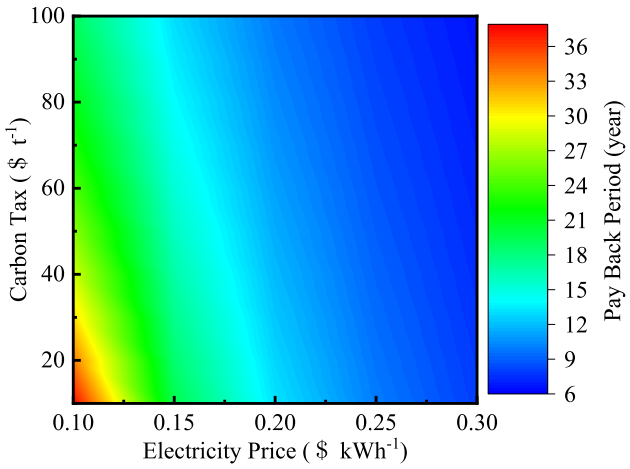

Fig. 12. Payback period of the optimized system under different electricity prices and carbon taxes.

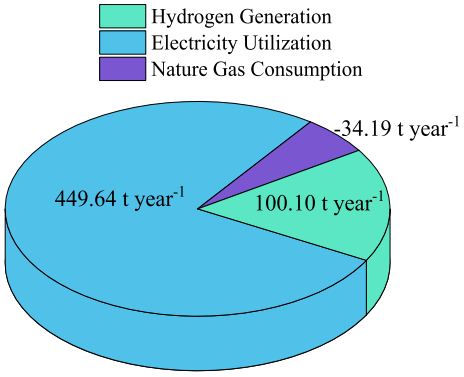

Fig. 13. *CDRR* proportion of the optimal system.

In the optimized system, lots of renewable energy can be utilized and a big amount of CO_2 emission is reduced. Fig. 13 shows the *CDRR* proportion of the optimal system. Scenario 3 is chosen and a small amount of CO_2 (34.19 t year^{-1}) will be emitted due to the consumption of natural gas via ICE. Meanwhile, the direct utilization of solar and wind energy and the generation of hydrogen via excess power can reduce a lot of CO_2 emissions, which can be 449.64 t year^{-1} and 100.10 t year^{-1}. Under the influence of these three aspects, the V2μG network's annual *CDRR* is 515.56 t year^{-1}.

To further show the effects of FCEV introduction and the designed strategy on degradation and efficiency performances of the V2μG network, the optimal system is compared with three reference systems by considering λ, $C.V_{deg}$, and $\eta_{ele,\ tot}$ in Fig. 14. The differences between the optimal system and reference systems are that reference system 2 has no FCEV, reference system 3 does not use the designed strategy of this research, and reference system 4 has neither FCEV nor the strategy design. Compared to reference system 4, the optimal system can reduce V2G-related equivalent battery ageing cycles, λ, from 14.52 cycles/year to 12.65 cycles/year, which accounts to a battery degradation reduction rate of 13%. The optimal system can also improve the $\eta_{ele,\ tot}$ from 12.92% to 15.30% (accounting a growth of 18%). Meanwhile, the $C.V_{deg}$ which reflects the uniformity of degradation distribution can be decreased from 0.159 to 0.032, showing the ability to control the distribution of the V2μG network. The performance improvements of the optimal system are achieved by the FCEV introduction and the design of the corresponding strategy. The effect of strategy design can be regarded as the differences between reference systems 2 and 4, where the λ decreases by 8.5% due to the reduction of energy flow between BEVs. However, as discussed in section 3, the use of the novel strategy will lead to an energy surplus, and the surplus electricity will continue to be

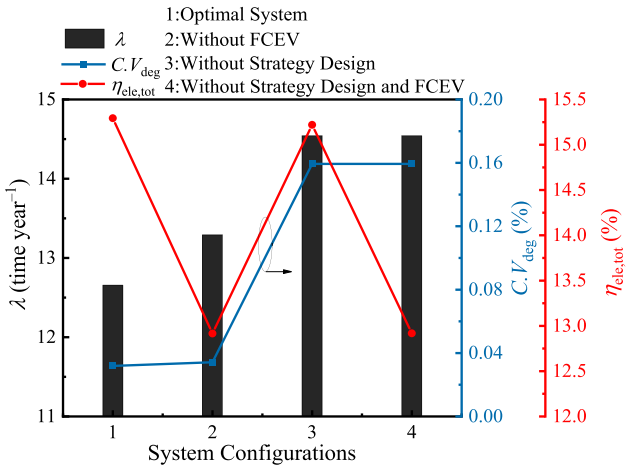

Fig. 14. Comparison of the optimal system and reference systems on λ, $C.V_{deg}$, and $\eta_{ele,\ tot}$.

stored in BEVs, which will reduce the role of the operation of designing the suitable SOC for each BEV. The introduction of FCEV can further improve the flexibility of the V2μG network energy utilization by converting the energy surplus into the chemical energy of hydrogen. Compared to reference system 2, the λ of the optimal system has a drop of 4.5% to be 12.65 cycles/year. It should be noted that the introduction of FCEV without the corresponding strategy design (from reference systems 4 to 3) can only increase energy efficiency through decreasing the energy loss without decreasing the λ because the electricity used for electrolysis is the electricity that cannot be stored by BEVs.

5. Conclusions

This paper proposes a new concept of 'Vehicle-to-Micro-Grid (V2μG) network' that incorporates the off-grid building energy system with flexible power storage/supply provided by battery EVs (BEVs) and fuel cell EVs (FCEVs). An energy management strategy is developed to exploit the potential of mitigating and homogenizing the battery degradation in BEVs by introducing different numbers of FCEVs to the off-grid system. The performances of the proposed V2μG network including technical, economic, environmental, and battery degradation, are comprehensively evaluated with different design and control parameter settings. The optimum system is attained with the NSGA-II algorithm and is compared with the conventional CCHP system based on internal combustion engines. The conclusions drawn from this study are as follows.

- For the studied scenarios, the proposed V2μG network can reduce and balance the battery degradation of the connected BEVs through the introduction of FCEVs which provide additional and flexible energy storage and supply for the V2μG network so that the charging/discharging of the connected EVs can be scheduled and managed.
- With the proposed energy management strategy, which simultaneously optimizes power distribution, start/stop of the backup power unit, and battery SOC of the connected EVs, the component degradation of the proposed V2μG network can be mitigated.
- For the optimal V2μG network obtained in this study, *CDRR* and *LCOE* can be 515.56 t year^{-1} and 0.104 \$ kWh^{-1} respectively with a surplus of 2495.5 kg hydrogen in one year. The additional battery degradation caused by the V2G service is 13% lower than that of the reference systems, and the $C.V_{deg}$ decreases from 0.159 to 0.032, showing the ability to control the degradation distribution of the proposed V2μG network.
- There is a trade-off between *CDRR* and *LCOE* when optimizing the crucial parameters of the proposed V2 μG network. By decreasing the capacities of the electrolyzer or REPG, more power will be supplied by ICE so that a lower *LCOE* of 0.054 \$ kWh^{-1} can be achieved. On the contrary, increasing the capacities of REPG and HG can achieve the CO_2 emissions reduction as high as 834.14 tons annually when compared to the off-grid system driven by internal combustion engines.

CRediT authorship contribution statement

Bingzheng Wang: Conceptualization, Methodology, Investigation, Writing – original draft. **Xiaoli Yu:** Investigation, Formal analysis, Funding acquisition. **Hongming Xu:** Conceptualization, Writing – review & editing, Funding acquisition. **Qian Wu:** Data curation, Formal analysis. **Lei Wang:** Data curation, Software. **Rui Huang:** Project administration. **Zhi Li:** Conceptualization, Writing – review & editing, Supervision. **Quan Zhou:** Conceptualization, Writing – review & editing, Funding acquisition.

Declaration of Competing Interest

The authors declare that they have no known competing financial interests or personal relationships that could have appeared to influence the work reported in this paper.

Data availability

Data will be made available on request.

Acknowledgements

This study has been funded by the National Natural Science Foundation of China (Grant No. 51976176) and the Open Fund Project from the State Key Laboratory of Clean Energy Utilization (No. ZJUCEU2021019).

Appendix A. Supplementary data

Supplementary data to this article can be found online at https://doi.org/10.1016/j.apenergy.2022.119873.

References

[1] Huo Y, Li P, Ji H, Yan J, Song G, Wu J, et al. Data-Driven Adaptive Operation of Soft Open Points in Active Distribution Networks. IEEE Trans Ind Inf 2021;17:8230–42.
[2] Huo Y, Li P, Ji H, Yu H, Yan J, Wu J, et al. Data-driven Coordinated Voltage Control Method of Distribution Networks with High DG Penetration. IEEE Trans Power Syst 2022:1.
[3] Bai Z, Liu Q, Gong L, Lei J. Application of a mid-/low-temperature solar thermochemical technology in the distributed energy system with cooling, heating and power production. Appl Energy 2019;253:113491.
[4] Sameti M, Haghighat F. Integration of distributed energy storage into net-zero energy district systems: Optimum design and operation. Energy 2018;153:575–91.
[5] Cho H, Smith AD, Mago P. Combined cooling, heating and power: A review of performance improvement and optimization. Appl Energy 2014;136:168–85.
[6] Bai Z, Liu T, Liu Q, Lei J, Gong L, Jin H. Performance investigation of a new cooling, heating and power system with methanol decomposition based chemical recuperation process. Appl Energy 2018;229:1152–63.
[7] Chang J, Li Z, Huang Y, Yu X, Jiang R, Huang R, et al. Multi-objective optimization of a novel combined cooling, dehumidification and power system using improved M-PSO algorithm. Energy 2022;239:122487.
[8] Kennedy KM, Ruggles TH, Rinaldi K, Dowling JA, Duan L, Caldeira K, et al. The role of concentrated solar power with thermal energy storage in least-cost highly reliable electricity systems fully powered by variable renewable energy. Adv Appl Energy 2022;6:100091.
[9] Song Z, Liu T, Liu Y, Jiang X, Lin Q. Study on the optimization and sensitivity analysis of CCHP systems for industrial park facilities. Int J Electr Power Energy Syst 2020;120:105984.

[10] Shirazi A, Taylor RA, Morrison GL, White SD. Solar-powered absorption chillers: A comprehensive and critical review. Energy Convers Manage 2018;171:59–81.
[11] Ji H, Chen S, Yu H, Li P, Yan J, Song J, et al. Robust operation for minimizing power consumption of data centers with flexible substation integration. Energy 2022;248:123599.
[12] Li Z, Lu Y, Huang R, Chang J, Yu X, Jiang R, et al. Applications and technological challenges for heat recovery, storage and utilisation with latent thermal energy storage. Appl Energy 2021;283:116277.
[13] Liu J, Chen X, Cao S, Yang H. Overview on hybrid solar photovoltaic-electrical energy storage technologies for power supply to buildings. Energy Convers Manage 2019;187:103–21.
[14] Xu Y, Zhang H, Yang F, Tong L, Yang Y, Yan D, et al. Experimental study on small power generation energy storage device based on pneumatic motor and compressed air. Energy Convers Manage 2021;234:113949.
[15] Jing R, Zhou Y, Wu J. Electrification with flexibility towards local energy decarbonization. Advances in Applied Energy 2022;5:100088.
[16] Song W, Zhang X, Tian Y, Xi L-H. A charging management-based intelligent control strategy for extended-range electric vehicles. Journal of Zhejiang University SCIENCE A 2016;17:903–10.
[17] Wang H, Hao Y, Kong H. Thermodynamic study on solar thermochemical fuel production with oxygen permeation membrane reactors. Int J Energy Res 2015;39:1790–9.
[18] Zhou Q, Li Y, Zhao D, Li J, Williams H, Xu H, et al. Transferable representation modelling for real-time energy management of the plug-in hybrid vehicle based on k-fold fuzzy learning and Gaussian process regression. Appl Energy 2022;305:117853.
[19] World Energy Outlook 2021. International Energy Agency; 2021). https://www.iea.org/reports/world-energy-outlook-2021 [accessed December 26, 2021].
[20] Miguel CV, Mendes A, Madeira LM. Intrinsic kinetics of CO_2 methanation over an industrial nickel-based catalyst. J CO2 Util 2018;25:128–36.
[21] Liu J, Cao S, Chen X, Yang H, Peng J. Energy planning of renewable applications in high-rise residential buildings integrating battery and hydrogen vehicle storage. Appl Energy 2021;281:116038.
[22] Zhou B, Li W, Chan KW, Cao Y, Kuang Y, Liu Xi, et al. Smart home energy management systems: Concept, configurations, and scheduling strategies. Renew Sustain Energy Rev 2016;61:30–40.
[23] Gilleran M, Bonnema E, Woods J, Mishra P, Doebber I, Hunter C, et al. Impact of electric vehicle charging on the power demand of retail buildings. Adv Appl Energy 2021;4:100062.
[24] Zhang H, Chen J, Yan J, Song X, Shibasaki R, Yan J. Urban power load profiles under ageing transition integrated with future EVs charging. Adv Appl Energy 2021;1:100007.
[25] Sedighizadeh M, Esmaili M, Mohammadkhani N. Stochastic multi-objective energy management in residential microgrids with combined cooling, heating, and power units considering battery energy storage systems and plug-in hybrid electric vehicles. J Cleaner Prod 2018;195:301–17.
[26] Yuan X, Liu Y, Bucknall R. Optimised MOPSO with the grey relationship analysis for the multi-criteria objective energy dispatch of a novel SOFC-solar hybrid CCHP residential system in the UK. Energy Convers Manage 2021;243:114406.
[27] Monforti Ferrario A, Bartolini A, Segura Manzano F, Vivas FJ, Comodi G, McPhail SJ, et al. A model-based parametric and optimal sizing of a battery/hydrogen storage of a real hybrid microgrid supplying a residential load: Towards island operation. Adv Appl Energy 2021;3:100048.
[28] Zhou Q, Li J, Shuai B, Williams H, He Y, Li Z, et al. Multi-step reinforcement learning for model-free predictive energy management of an electrified off-highway vehicle. Appl Energy 2019;255:113755.
[29] Alsharif A, Tan CW, Ayop R, Dobi A, Lau KY. A comprehensive review of energy management strategy in Vehicle-to-Grid technology integrated with renewable energy sources. Sustainable Energy Technol Assess 2021;47:101439.
[30] Shi R, Li S, Zhang P, Lee KY. Integration of renewable energy sources and electric vehicles in V2G network with adjustable robust optimization. Renew Energy 2020;153:1067–80.
[31] Farahani SS, Bleeker C, van Wijk A, Lukszo Z. Hydrogen-based integrated energy and mobility system for a real-life office environment. Appl Energy 2020;264:114695.
[32] Liu J, Yang H, Zhou Y. Peer-to-peer trading optimizations on net-zero energy communities with energy storage of hydrogen and battery vehicles. Appl Energy 2021;302:117578.
[33] Ji H, Jian J, Yu H, Ji J, Wei M, Zhang X, et al. Peer-to-Peer Electricity Trading of Interconnected Flexible Distribution Networks Based on Distributed Ledger. IEEE Trans Ind Inf 2022;18:5949–60.
[34] Child M, Nordling A, Breyer C. The impacts of high V2G participation in a 100% renewable Åland energy system. Energies 2018;11:2206.
[35] Bishop JD, Axon CJ, Bonilla D, Tran M, Banister D, McCulloch MD. Evaluating the impact of V2G services on the degradation of batteries in PHEV and EV. Appl Energy 2013;111:206–18.
[36] Thingvad A, Calearo L, Andersen PB, Marinelli M. Empirical Capacity Measurements of Electric Vehicles Subject to Battery Degradation from V2G Services. IEEE Trans Veh Technol 2021;70:7547–57.
[37] Dubarry M, Devie A, McKenzie K. Durability and reliability of electric vehicle batteries under electric utility grid operations: Bidirectional charging impact analysis. J Power Sources 2017;358:39–49.
[38] Marongiu A, Roscher M, Sauer DU. Influence of the vehicle-to-grid strategy on the aging behavior of lithium battery electric vehicles. Appl Energy 2015;137:899–912.
[39] Wang B, Yu X, Chang J, Huang R, Li Z, Wang H. Techno-economic analysis and optimization of a novel hybrid solar-wind-bioethanol hydrogen production system via membrane reactor. Energy Convers Manage 2022;252:115088.
[40] Hernández B, Martín M. Optimal production of syngas via super-dry reforming. Analysis for natural gas and biogas under different CO_2 taxes. Chem Eng Res Des 2019;148:375–92.
[41] Chen C, Lu Y, Xing L. Levelling renewable power output using hydrogen-based storage systems: a techno-economic analysis. J Storage Mater 2021;37:102413.
[42] Neupane D, Kafle S, Karki KR, Kim DH, Pradhan P. Solar and wind energy potential assessment at provincial level in Nepal: Geospatial and economic analysis. Renewable Energy 2022;181:278–91.
[43] Xie Y, Cui Y, Wu D, Zeng Y, Sun L. Economic analysis of hydrogen-powered data center. Int J Hydrogen Energy 2021;46:27841–50.
[44] Gallardo FI, Ferrario AM, Lamagna M, Bocci E, Garcia DA, Baeza-Jeria TE. A Techno-Economic Analysis of solar hydrogen production by electrolysis in the north of Chile and the case of exportation from Atacama Desert to Japan. Int J Hydrogen Energy 2021;46:13709–28.
[45] Wang H, Wang B, Qi X, Wang J, Yang R, Li D, et al. Innovative non–oxidative methane dehydroaromatization via solar membrane reactor. Energy 2021;216:119265.
[46] Hamzehkolaei FT, Amjady N. A techno-economic assessment for replacement of conventional fossil fuel based technologies in animal farms with biogas fueled CHP units. Renewable Energy 2018;118:602–14.
[47] Zhang J, Cao S, Yu L, Zhou Y. Comparison of combined cooling, heating and power (CCHP) systems with different cooling modes based on energetic, environmental and economic criteria. Energy Convers Manage 2018;160:60–73.
[48] Kong L, Li L, Cai G, Liu C, Ma P, Bian Y, et al. Techno-economic analysis of hydrogen energy for renewable energy power smoothing. Int J Hydrogen Energy 2021;46:2847–61.
[49] Electricrate. Pricing of Electricity by Country. https://www.electricrate.com/data-center/electricity-prices-by-country/. [accessed June 29, 2022].
[50] Wang S, Zhang N, Li Z, Shahidehpour M. Modeling and impact analysis of large scale V2G electric vehicles on the power grid. IEEE PES Innovative Smart Grid Technologies. IEEE; 2012. pp. 1-6.
[51] Zhou Q, He Y, Zhao D, Li J, Li Y, Williams H, et al. Modified particle swarm optimization with chaotic attraction strategy for modular design of hybrid powertrains. IEEE Trans Transp Electrif 2020;7:616–25.
[52] Araújo DR, Bastos-Filho CJ, Barboza EA, Chaves DA, Martins-Filho JF. A performance comparison of multi-objective optimization evolutionary algorithms for all-optical networks design. 2011 IEEE Symposium on Computational Intelligence in Multicriteria Decision-Making (MDCM). IEEE; 2011. pp. 89-96.
[53] Jing R, Zhu X, Zhu Z, Wang W, Meng C, Shah N, et al. A multi-objective optimization and multi-criteria evaluation integrated framework for distributed energy system optimal planning. Energy Convers Manage 2018;166:445–62.
[54] Zhou Q, Zhao D, Shuai B, Li Y, Williams H, Xu H. Knowledge implementation and transfer with an adaptive learning network for real-time power management of the plug-in hybrid vehicle. IEEE Trans. Neural Netw. Learn. Syst. 2021;32(12):5298–308. https://doi.org/10.1109/TNNLS.2021.3093429. In this issue.